Final Draft
of the original manuscript:

Dobrynin, M.; Gayer, G.; Pleskachevsky, A.; Guenther, H.**:**
Effect of waves and currents on the dynamics and seasonal variations of suspended particulate matter in the North Sea
In: Journal of Marine Systems (2010) Elsevier

DOI: 10.1016/j.jmarsys.2010.02.012

Effect of waves and currents on the dynamics and seasonal variations of suspended particulate matter in the North Sea

Mikhail Dobrynin[a,*], Gerhard Gayer[a], Andrey Pleskachevsky[a], Heinz Günther[a]

[a] *GKSS Research Centre, Institute for Coastal Research, Max-Planck-Straße 1, 21502, Geesthacht, Germany*

Abstract

Effect of waves and currents on the dynamics and seasonal variations of suspended particulate matter (SPM) in the North Sea is investigated by a three-dimensional Circulation and Transport Model for SPM (CTM-SPM) in 2002 and 2003, forced by waves and meteorological data. Calculated fine sediment exchange processes at the seawater-seabed interface are driven by the instant values of the shear stress velocity due to currents and waves. Modeled SPM concentrations are compared with in-situ measurements and satellite snap-shot images. As a result of the action of currents and waves, local bathymetry and the fine sediment content at the sea bottom, modeled time series show different short-term dynamics of SPM concentrations in various locations in the North Sea. On a longer time scale, currents and waves result in different seasonal distributions of the shear stress velocity typical for the calm (April – October) and the storm (October – April) periods. Accordingly, our model calculates different seasonal distributions of SPM with the mean surface concentrations of about 2 mg l^{-1} in the calm and > 5 mg l^{-1} in the storm periods. Waves lead to a higher frequency of resuspension and erosion events and increase mixing intensity in the water column during storm periods. During calm periods, SPM distribution is mainly shaped by currents. A different pattern, characterized by high SPM concentrations in offshore areas, evolves instantly during transient storms events.

Key words: suspended particulate matter, seasonal variations, dynamics, modeling, North Sea, satellite data

1. Introduction

In the North Sea, the combination of topography, hydrographic and weather conditions, together with abundant sources makes suspended particulate matter (SPM) an integral and important part of marine ecosystem. Its distribution in the water column influences the plankton primary production by regulating the light penetration depth in seawater (Reid et al., 1990). SPM can also absorb and transport some human-made contaminants, such as heavy metals (Haarich et al., 1993), persistent organic pollutants (Ilyina et al., 2006) and radionuclides (Nies et al., 1999). Furthermore, knowledge about transport, erosion and deposition of fine sediment in morphodynamic systems is necessary for the construction of coastal protection structures, mining of sand and dredging of navigation channels (de Swart and Calvete, 2003). The visible effect of SPM processes is a change in seawater color from blue to yellow (Jonasz and Fournier, 2007) depending on the SPM concentration occurring under different ambient conditions.

SPM in the model is defined as fine solid inorganic particles suspended in water, which originate mostly from the fine sediment (mud) in the bottom and fluvial inflow. It is classified by the grain size (Wentworth, 1922; Krumbein and Sloss, 1963), referred to as fine sediment fractions. The most abundant are silt ($4 - 63$ μm) and clay (< 4 μm). There are also larger (and heavier) fractions (> 63 μm), such as sand or gravel.

*Corresponding author. Present address: Danish Meteorological Institute, Lyngbyvej 100, DK-2100 Copenhagen, Denmark. Tel.: +45 3915 7385

Email addresses: mdo@dmi.dk (Mikhail Dobrynin)

They are rarely eroded from the seabed and rapidly sink back. On the contrary, the very fine fraction (< 1 μm) remains in suspension in water for a long time.

Fine sediment exchange processes at the seabed-water interface, i.e. resuspension, erosion and sedimentation have stepwise character depending on the intensity of turbulence in the near-bottom layer caused by waves and currents which can be expressed by the shear stress velocity. In many models, SPM exchange processes are controlled by threshold values of the shear stress velocity (Sündermann and Puls, 1990; Pohlmann and Puls, 1994; Puls et al., 1997; Gayer et al., 2006). Bed shear stress is a driving forcing factor for suspended sediment dynamics in the southern North Sea (Stanev et al., 2009). However, SPM models commonly use temporally averaged currents velocity and wave parameters and, as a result, smooth and suppress the magnitude of modeled processes governing the distribution of SPM. Such approach leads to the decrease in the intensity of SPM seabed-water mass exchange and underestimates the role of the seabed in the SPM burden in the model. In this study, we use instant values of shear stress velocity in order to better resolve the stepwise character of SPM exchange. This is achieved by embedding the SPM processes into a three-dimensional circulation and transport model.

Spatial resolution also plays an important role in the modeling of SPM dynamics. Comparison between the circulation model results obtained using a meso-scale (3 km) and a large-scale (20 km) horizontal resolution showed that not only the temperature and salinity distributions, but also kinetic energy is strongly affected by the chosen grid cell size (Pohlmann, 2006). Fine spatial resolution is particularly important in the shallow and coastal regions where the SPM content is high and SPM dynamics is intensive (Seifert et al., 2009). Previous modeling studies (e.g. Gayer et al. (2006)) focused only on the discrete time intervals (a few weeks) and did not cover longer time periods. Such calculations do not display seasonal variations in the SPM dynamics.

We performed continuous calculations of SPM dynamics in the North Sea with the fine spatial resolution of 2.5' by 1.5' in the years 2002 and 2003. Some model processes (i.e. bioturbation) were refined compared to previous model experiments (Gayer et al., 2006). We evaluated modeled SPM concentrations against in-situ measurements of SPM. Additionally, instant values of SPM concentrations were compared with snap-shot satellite data, because satellite images reflect phenomena involved in the SPM dynamics, i.e. river plumes, coastal and seabed erosion under storm conditions and SPM fronts.

Waves and currents have principally different roles in the vertical dynamics of SPM. Vertical distributions of SPM in the North Sea vary from full mixing over the entire water column generally induced by the waves, to strong stratified structure with high gradients of SPM concentration mainly shaped by currents. Therefore, the main focus of our study was on the analysis of the relative impact of currents and waves on the horizontal and vertical distribution of SPM in the North Sea and its seasonal variations.

2. Method description

2.1. Description of processes included in the model

The three-dimensional Circulation and Transport Model for Suspended Particulate Matter (CTM-SPM) was designed to describe the long-term dynamics of SPM in the North Sea. CTM-SPM is based on the existing, improved and newly developed modeling tools and consists of three major components.

- The ocean circulation module is based on the model HAMSOM (Backhaus, 1985; Pohlmann, 1996).
- The SPM module adopted from the GKSS-BSH SPM model (Gayer et al., 2006).
- The newly developed fine sediment bioturbation module based on the diffusion equation (Appendix B).

All modules are embedded into the same code and are integrated with the time step of 5 minutes. This ensures that the SPM dynamics is calculated based on the instant values of currents.

SPM in the model is represented by solid, round inorganic particles suspended in seawater. These particles differ in sources and size and are treated in the model as separate fractions with different properties. The SPM-related processes included in the model can be grouped under four categories:

1. Transport with ocean currents due to advection and turbulent diffusion (Section 2.1.1).
2. Vertical processes in the water column including gravitational sinking and transport by vertical components of turbulent diffusion and advection (Section 2.1.2).
3. Seabed-water exchange processes which take place in both directions as a result of sedimentation, resuspension and erosion (Section 2.1.3).
4. Seabed processes, such as bioturbation, which is a primary cause for SPM redistribution in the upper sediment (Section 2.1.4).

2.1.1. SPM transport with ocean currents

SPM in water results from the sum of sources, sinks, and is transported by the flow field. SPM is advected by currents forced by wind stress, horizontal and vertical water density gradients, as well as by the predominant semidiurnal lunar tide M2. Behaviour of SPM with the concentration C and the sources-sink term Q_C is described by:

$$\frac{\partial C}{\partial t} = \frac{\partial}{\partial x}\left(Av_x \frac{\partial C}{\partial x}\right) + \frac{\partial}{\partial y}\left(Av_y \frac{\partial C}{\partial y}\right) + \frac{\partial}{\partial z}\left(Av_z \frac{\partial C}{\partial z}\right) - \left(u\frac{\partial C}{\partial x} + v\frac{\partial C}{\partial y} + w\frac{\partial C}{\partial z}\right) + Q_C\,(t, x, y, z) \tag{1}$$

Horizontal advection of SPM is calculated using components of the flow field in the eastern and northern directions (u and v). Flow components u and v, as well as the horizontal turbulent diffusion coefficients (Av_x and Av_y) are calculated in the circulation module (HAMSOM). The vertical component of the flow field (w) is calculated from u and v using the continuity equation. The vertical turbulent diffusion coefficient Av_z is calculated as described in Section 2.1.2.

The three-dimensional, baroclinic, primitive equation model HAMSOM (Hamburg Shelf Ocean Model) includes the equations of motion and continuity, the equation of state for seawater, as well as transport equations for temperature and salinity. HAMSOM used a semi-implicit scheme for the shallow water equations. The only constraint on the time step required to keep the semi-implicit scheme stable is that associated with gravity-wave propagation. This schema is most relevant for long-term simulations and provides realistic results for time periods of decades. The detailed description of HAMSOM is given in Backhaus (1985) and Pohlmann (1996). The model has been applied and validated for different shelf regions in the world, such as for example the North Sea, the Baltic Sean, the South China Sea and the Bohai Sea (Backhaus and Hainbucher, 1987; Pohlmann, 1996; Huang et al., 1999).

2.1.2. Vertical processes in the water column

Gradients of current velocity and water perturbations at the surface due to wind stress and waves determine turbulence in the North Sea. In the near seabed water layers turbulence occurs due to bottom friction. Vertical turbulent diffusion and the vertical component of advection distribute SPM in the water column. The vertical diffusion coefficient Av_z ($\mathrm{m^2\ s^{-1}}$) is composed by two components describing the action of waves (Av_{wave}, $\mathrm{m^2\ s^{-1}}$) and ocean currents (Av_{cur}, $\mathrm{m^2\ s^{-1}}$). The contribution of ocean currents into Av_{cur} can be calculated from the equation which describes the currents speed shear in the neighboring layers (Pleskachevsky et al., 2005).

$$\frac{dU}{dz} = \frac{Av_{cur}}{K_P^2} \tag{2}$$

The diffusivity coefficient $K_P = U^2/g$ is the Prandl's mixing length (m) with the current velocity U ($\mathrm{m\ s^{-1}}$) and gravitational acceleration g ($\mathrm{m\ s^{-2}}$).

Additionally, the contribution of waves Av_{wave} ($\mathrm{m^2\ s^{-1}}$; Pleskachevsky et al. (2005)) represents the kinetic energy of waves calculated as a function of significant wave height H_s (m), wave number k ($\mathrm{m^{-1}}$), peak period T (s) and the maximum orbital wave velocity U_w ($\mathrm{m\ s^{-1}}$).

$$Av_{wave} = (k \cdot H_s)^2 \cdot U_w^2 \cdot T \tag{3}$$

The change in SPM concentration due to gravitational sinking C_{sink} (kg m^{-3}) over the time step Δt is calculated using the actual concentrations of SPM C (kg m^{-3}) in each model layer with the thickness h (m) and a sinking velocity W_{sink} (m s^{-1}).

$$\frac{\partial C_{sink}}{\partial t} = C\frac{W_{sink}}{h} \tag{4}$$

For the entire water column, the SPM concentration in each layer increases due to sinking from the layer above and decreases due to sinking into the layer below.

2.1.3. Exchange processes at the seabed-water interface

The intensity of turbulence due to waves and currents in the near-bottom water layer is represented in the model by the shear stress velocity V^* (m s^{-1}; see Appendix A). It drives the exchange processes between the water and the seabed according to the threshold values for sedimentation, resuspension and erosion. The choice of the threshold values for V^* is based on the analysis of the measured and experimental data for the German Bight (located in the south-eastern part of the North Sea) and the North Sea described in Pohlmann and Puls (1994) and Gayer et al. (2006). In this study, the following values are used:

sedimentation	V^*	$<$	V^*_{sed}	$=$	0.99 cm s^{-1}
resuspension	V^*	$>$	V^*_{res}	$=$	1.00 cm s^{-1}
erosion	V^*	$>$	V^*_{ero}	$=$	2.80 cm s^{-1}

Sedimentation starts when conditions in the near-bottom water layer are calm and V^* drops below the threshold value V^*_{sed} . It decreases the SPM content in the lowest water layer and increases the fine sediment mass in the upper seabed layer. The change of SPM mass per unit area M_{sed} (kg m^{-2}) over the time Δt (s) is calculated as:

$$\frac{\partial M_{sed}}{\partial t} = C_b \cdot W_{sink}\left(1 - (V^*/V^*_{sed})^2\right) \tag{5}$$

with C_b (kg m^{-3}) being the actual SPM concentration in the bottom water layer.

Resuspension occurs when V^* exceeds the threshold value V^*_{res} . Then, the total mass content of the upper seabed layer is resuspended into the bottom water layer.

Erosion starts when V^* exceeds the threshold value V^*_{ero} . The fine sediment mass is completely removed from the seabed layers down to the depth of erosion h_{ero} (m; see for example Fig. 7).

$$h_{ero} = k_{ero}(V^{*2} - -V^{*2}_{ero})/V^{*2}_{ero} \tag{6}$$

Experimental coefficient $k_{ero} = 0.001$ m is adjusted to represent conditions typical for the North Sea for sediment fractions up to 63 μm (Pleskachevsky et al., 2005).

2.1.4. Seabed processes

The sediment compartment in the model is represented by the upper 20 cm of the seabed. Differing from the approach used by Gayer et al. (2006), which assumes a constant bioturbation rate, CTM-SPM includes seasonally and spatially variable bioturbation in the seabed. Exchange within the sediment compartment due to biotic activity is modeled by a diffusion equation with a coefficient for bioturbation Av_{bio} (m^2 s^{-1})

$$\frac{\partial M}{\partial t} = \frac{\partial}{\partial z}\left(Av_{bio}\frac{\partial M}{\partial z}\right) \tag{7}$$

To simulate the effect of bioturbation, the value of Av_{bio} is calculated for each model grid point depending on the season s_f, location l_f, and depth in the bottom h_f.

$$Av_{bio} = Av^{max}_{bio} \cdot s_f \cdot l_f \cdot h_f \tag{8}$$

The Av^{max}_{bio} as well as the dimensionless factors of eq. 8 are described in Appendix B.

2.2. Model setup and forcing

We used a combination of ocean circulation model with an SPM transport module and a wave and atmospheric models (Fig. 1). Model simulation covers the southern North Sea from 50.87°N to 57.17°N and from 3.40°W to 9.10°E (Fig. 2) with a temporal resolution of 5 minutes for the time period of two years starting in the beginning of 2002 until the end of 2003. The year 2002 is used to analyze the instant processes governing the dynamics of SPM in details and to compare model results with available in-situ and satellite measurements. The seasonal analysis of forcing factors and the SPM distributions, and dynamics was performed for the years 2002 and 2003.

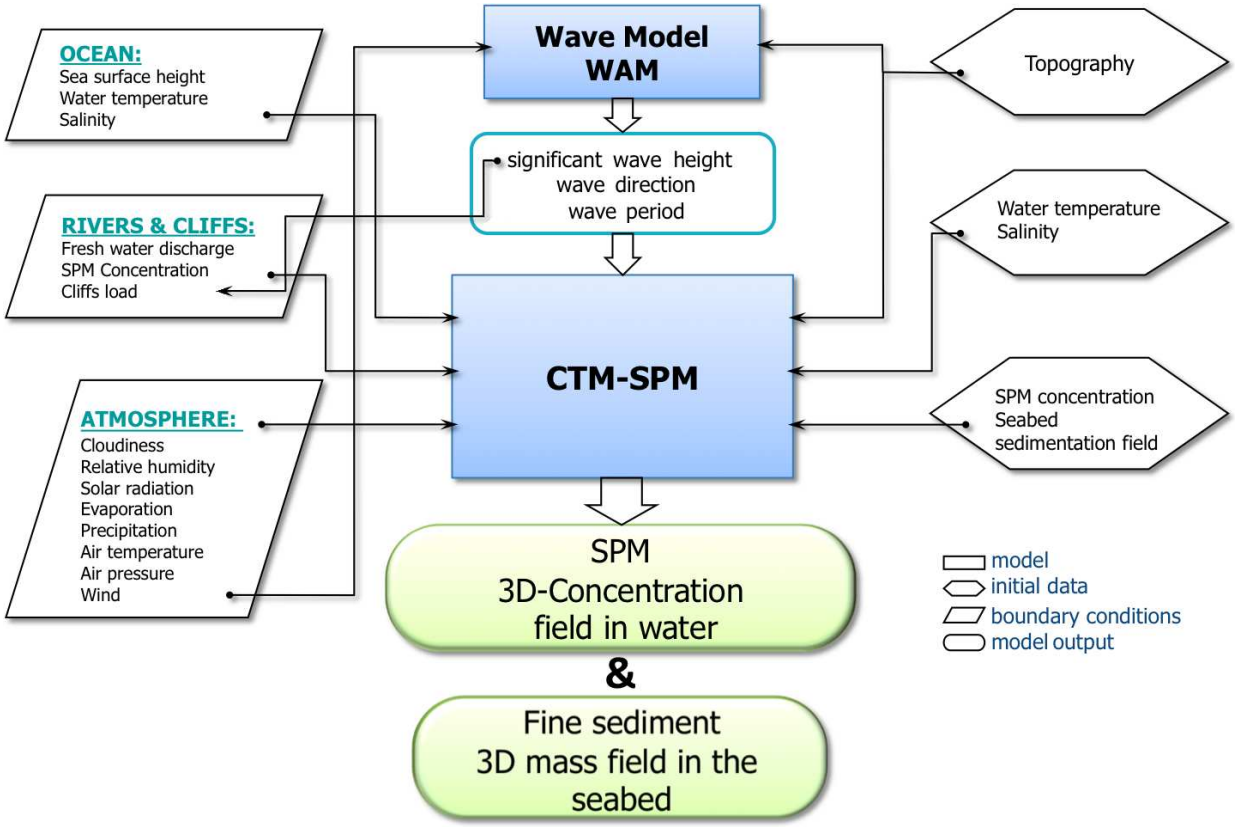

Figure 1: Model concept and data flow.

The model grid has a horizontal resolution of 1.5′ in the north-south direction and 2.5′ in the east-west direction (corresponding to about 2.5-3 km). The model has 21 vertical layers in water and 21 layers in the seabed. The model layers thickness in water varies from 5 m in the upper layers up to 10 m in the lower layers. The layers thickness in the seabed increases from 0.5 mm in the upper layers to 5 cm in the lower layers.

2.2.1. SPM fractions in the model

The SPM concentration in the model is represented by three fractions (SPM1, SPM2 and SPM3) with different particle size (K_{size}) and the sinking velocities (W_{sink}; see Table 1). There SPM fractions, ranging in grain size from < 20 μm to 63 μm are chosen so that they correspond to the grain sizes of the measured SPM in the North Sea (Eisma and Kalf, 1987). SPM1 and SPM2 fractions represent two different types of fine sediment with the grain size < 20 μm and different sinking velocity. SPM3 represents the larger SPM fraction with the grain size of 63 μm. The sinking velocities of fractions SPM1 and SPM2 are based on the measurements in the German Bight in January-February 1993 (Puls et al., 1995). The sinking velocity of

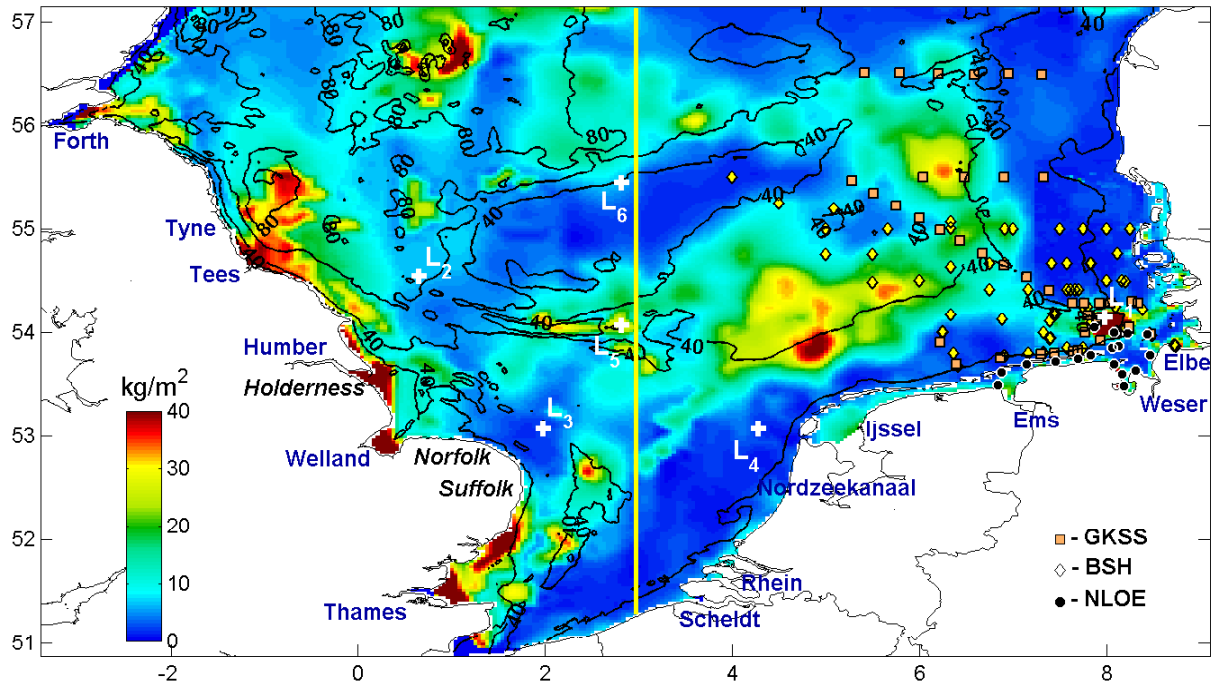

Figure 2: Model area, initial seabed distribution of fine sediment ($< 20\ \mu m$) fraction (colors in kg m^{-2}) and bathymetry (lines, depth in m) on a grid of 1.5′ by 2.5′. Geographical locations of points selected for time series analysis (L1, L2, L3, L4, L5 and L6 in Section 3), as well as points where measured SPM concentrations in water (color markers) were available for model evaluation are indicated. English cliffs (black italic labels) and rivers (blue labels) are shown. A line along 3°E shows vertical section referred to Fig. 7.

SPM3 fraction is calculated using the Stokes formula for silt grain with a size of 40 μm. SPM concentration in water, rivers, near cliffs, and on the open model boundaries is formed as a sum of these three fractions in different proportions (Table 1).

Table 1: Summary of SPM fractions. SPM particle size, sinking velocity and their content in the sources and in the seabed.

Fractions		SPM1	SPM2	SPM3
Particle size, $K_{size}(\mu m)$		< 20	< 20	20-63
Sinking velocity, W_{sink} (mm s^{-1})		0.10	0.02	1.00
Content [%]	North Atlantic	88.0	12.0	0.0
	English Channel	12.5	87.5	0.0
	English Cliffs	40.0	20.0	40.0
	Rivers, f_{riv}	25.0	50.0	25.0
	Seabed, f	80.0	20.0	–
Initial range in water (surface-lowers layers) (mg l^{-1})		0.5-5.0	0.1-1.0	0.05-0.5

2.2.2. Initial distribution of SPM in water and fine sediment in the seabed

Model calculations in water were initialized with the vertically integrated SPM concentrations that reproduce the typical SPM distribution in the North Sea during the calm period for each SPM fraction depending on the depth (Table 1). The initial SPM concentration forms the background distribution of SPM in water. In the beginning of the model simulation (the first few days), before the first strong mixing event, the vertical profile of SPM concentration in the water column as well as the resuspension layer in the

seabed are formed mainly by settling of SPM from the upper layers. This approach allows to capture the zones with high and low SPM contents in the North Sea in order to achieve more realistic SPM distributions before the first resuspension or erosion event occurs. After such a mixing event, all processes are fully involved in the SPM concentration integrations.

The seabed distributions of fine sediment fractions SPM1 and SPM2 are used to calculate the initial content of fine sediment in the seabed (Fig. 2). Initially, the fine sediment map was generated from the measured grain size data (Gayer et al., 2004). In the German Bight and in the eastern part of the North Sea, the map was improved based on the surface SPM concentrations retrieved from satellite data MOS (Modular Optical Spectrometer) and using the eroded SPM mass calculated by an SPM model (Pleskachevsky et al., 2005) as described in Appendix C. The three-dimensional initial sediment mass M (kg m^{-2}) in the seabed layer with the depth z_b (m) for the fractions SPM1 and SPM2 ($f_{1,2}$; Table 1) is calculated as:

$$M_{1,2} = f_{fine} \cdot f_{1,2} \cdot z_b \cdot \rho_{dry} \tag{9}$$

The best–fit function was estimated for fraction SPM3 based on the measurements in the German Bight (Koenig et al., 1994; Puls et al., 1995):

$$M_3 = 39 \cdot \sin\left(f_{fine}/32\right) \cdot z_b \cdot \rho_{dry} \tag{10}$$

The dry density of fine sediment in this study is $\rho_{dry} = 1300$ kg m^{-3}.

2.2.3. SPM concentrations in the rivers, cliffs and open boundaries

The seabed is the main source of SPM in North Sea which determines the SPM distribution in the water. Additional sources of SPM in the model are rivers, English cliffs (Fig. 3) and the open boundaries. The hourly fresh water discharges from the rivers Elbe, Weser, Ems and Rhine (DOD, 2006), the daily fresh water discharges from Ijssel, Nordzeekanaal and Scheldt (Pätsch and Lenhart, 2004), as well as climatological monthly mean discharges from the rivers Thames, Welland, Humber, Tees, Tyne and Forth (GRDC, 2006) are linearly interpolated to fit the temporal resolution of the model. The rivers load of SPM L_{riv} (kg s^{-1}; Fig. 3a, b) is calculated as the product of the fresh water discharge D_{riv} (m^3 s^{-1}) and the annual mean SPM concentration (Gayer et al., 2004) in each river C_{riv} (kg m^{-3}).

$$L_{riv} = D_{riv} \cdot C_{riv}. \tag{11}$$

The concentration change of SPM for each fraction due to rivers C_{riv} (kg m^{-3}) is calculated using the actual water volume Vol (m^3) in the grid cells where the rivers enter the model domain and content of the SPM fractions (f_{riv}) in the rivers load (see Table 1):

$$\frac{\partial C_{riv}}{\partial t} = f_{riv} \frac{L_{riv}}{Vol} \tag{12}$$

Note that in 2003, the fresh water discharge and SPM loads in the major rivers (i.e. Rhine, Elbe and Weser) were up to one order of magnitude lower compared to 2002 because of the extremely high temperatures and low precipitation rate in the central and western parts of Europe.

The contribution of the English cliffs into the SPM concentration (Fig. 3c) is based on the long-term measurements of annual mean amounts of eroded SPM from Suffolk (50 kg s^{-1}), Norfolk (45 kg s^{-1}) and Holderness (58 kg s^{-1}). The SPM loads from cliffs are calculated stepwise depending on whether storm or calm conditions occur (Fig. 3c). Storm conditions in the model start when significant wave heights near the coast are > 2 m, based on the three years wave-height statistics near cliffs (Gayer et al., 2006). Significant wave heights for the year 2002 and 2003 calculated by the wave model WAM are used to estimate the SPM load from cliffs (see Section 2.2.4 and Fig. 1).

Open boundary conditions are the sea surface elevation induced mainly by tides (obtained from the large-scale HAMSOM model domain for the North Atlantic) and climatological monthly mean values of the seawater temperature and salinity (Fig. 1).

SPM concentration at the open boundaries of the North Atlantic and the English Channel is assumed to be constant in time and vertically integrated over the water column with values of 5 and 8 mg l^{-1} respectively (Puls et al., 1997; Gayer et al., 2006). The distribution between the SPM fractions in the English cliffs and at the open boundaries is given in Table 1.

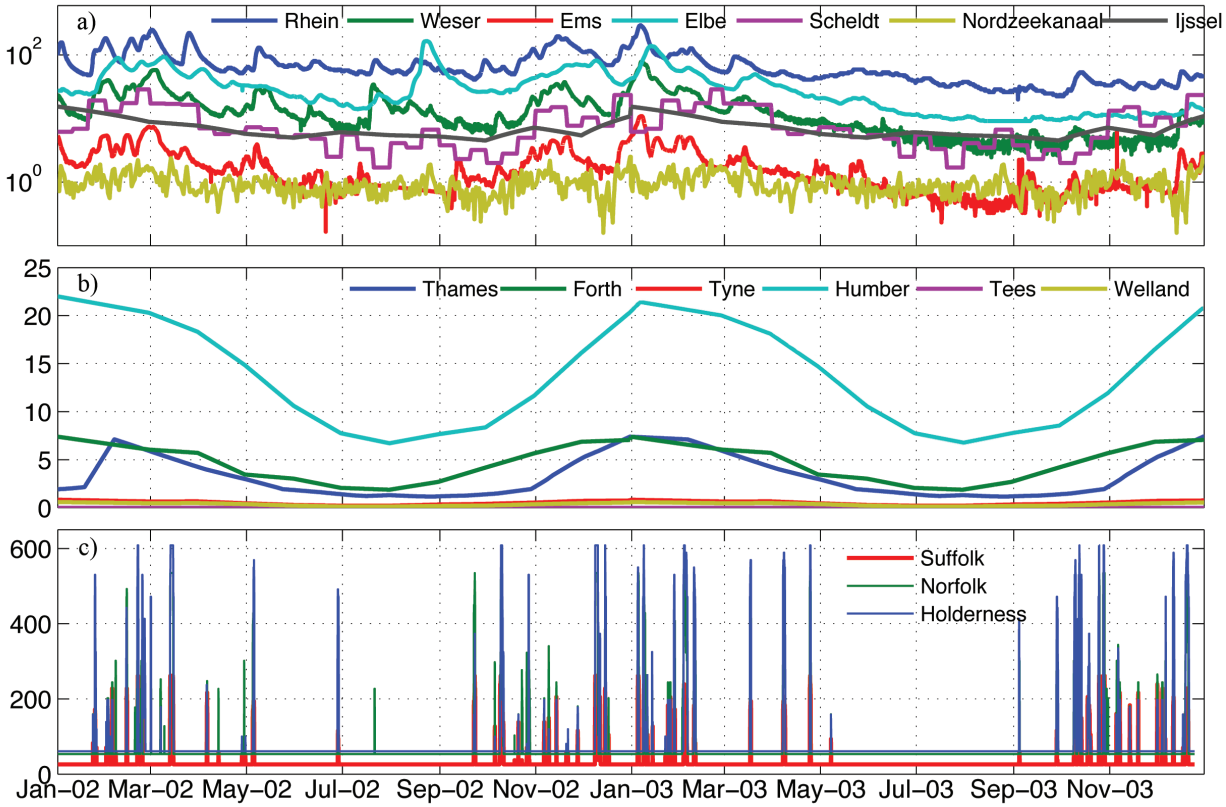

Figure 3: Loads of SPM (kg s^{-1}) to the North Sea in the continental (a), UK rivers (b) and English cliffs (c) in 2002 and 2003. Geographical locations are shown on the map (Fig. 2).

2.2.4. Meteorological and wave forcing

Meteorological forcing including the wind, atmospheric pressure, air temperature, relative humidity and cloudiness is based on the hourly data calculated by the Regional Model of atmosphere REMO (Feser et al., 2001). The REMO model is based on the primitive equations in a terrain-following hybrid coordinates system. The model has a resolution of 0.5° and model area from 50.0°W to 70.0°E and from 30.0°N to 77.50°N. REMO is forced with the NCEP reanalysis data (NCEP, 2005).

Wave forcing is calculated by the third-generation spectral ocean wave model WAM (Wave Analysis Model; WAMDI Group (1988); Günther et al. (1992); Komen et al. (1994)). The WAM model on a Cartesian grid in this study was first applied for the North Atlantic on a coarse grid forced by the wind filed from the NCEP re-analysis. Then it was applied for the southern North Sea with the depth-induced refraction option (on the same grid as the CTM-SPM model, nested in the coarse grid) forced by wind from the REMO data and using the boundary conditions from the WAM run for the North Atlantic. Significant wave heights, wave peak periods and wave directions represent the wave forcing in the CTM-SPM model.

2.3. Model setup verification

Hourly averaged modeled three-dimensional SPM concentrations in water and fine sediment mass in the seabed were calculated as the sum of three SPM fractions (see Section 2.2.1). We compared hourly averaged modeled concentration with in-situ measurements at the sea surface and in the water column. Water samples were collected during several cruises in 2002 in the eastern and south-eastern North Sea. Additionally, surface SPM concentrations averaged over 20 minutes were used for comparison with satellite snap-shot images from MERIS (MEdium-spectral Resolution, Imaging Spectrometer operating in the solar

reflective spectral range) and MOS (Modular Optical Spectrometer). Generally, model results are in good agreement with in-situ observations characterized by a correlation coefficient of $0.4-0.92$ and BIAS (model-measurements) of 3.1-5.5 mg l^{-1}. Spatial model resolution is coarser than the resolution of satellite data. As a result, modeled SPM surface distributions are smoothed and do not reproduce the finest details in the horizontal SPM patterns visible from satellite. More details on model results evaluation are given in Appendix D and E.

3. Temporal evolution of SPM concentrations

We analyzed temporal dynamics of modeled surface SPM concentrations in different locations in the years 2002 and 2003 (Fig. 4). In the locations L3, L4 and L5, the lowest surface SPM concentrations occurred in the summer time and the highest during the cold period. In the location L1 in the German Bight, the seasonality is not so pronounced because the currents component of shear stress velocity (mainly forced by M2 tide) dominates and does not change significantly from warm to cold period in this area (see Section 5.1). Shear stress and vertical mixing due to currents in the German Bight are strong enough to keep SPM in suspension. Daily averaged time series of surface SPM concentrations (Fig. 4) smooth the

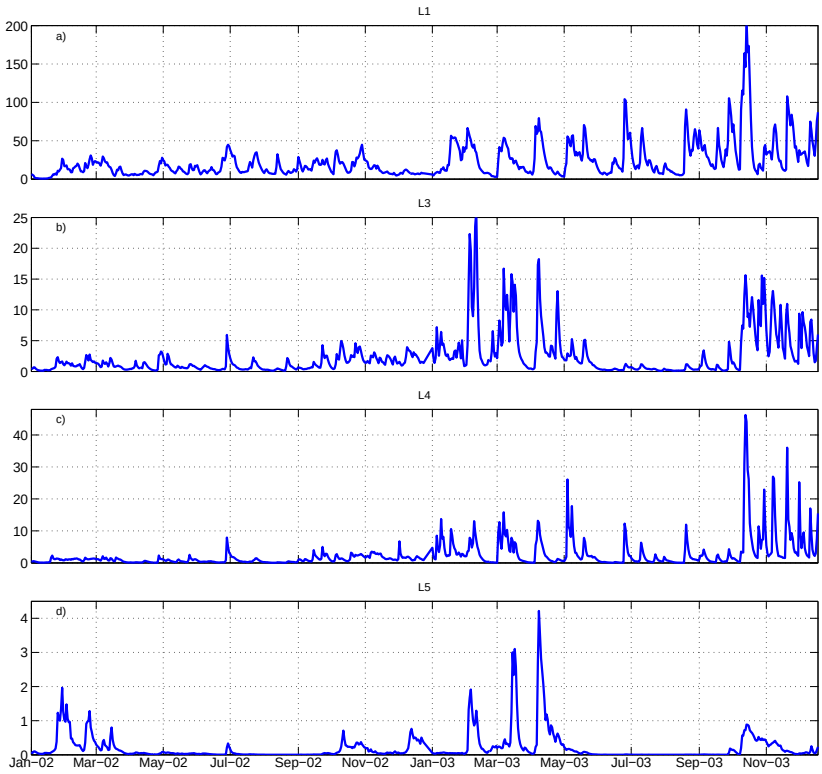

Figure 4: Time series of daily averaged surface SPM concentration (mg l^{-1}) in the locations L1, L3, L4 and L5 (see Fig. 2 for the geographical locations) in the years 2002 and 2003.

intencity in the instant SPM dynamics captured by the model. Therefore we also show time series at six selected locations in the year 2002 (Table 2) to demonstrate in details the different temporal evolution of SPM concentrations (Fig. 5 and Fig. 6) under different waves or currents regimes and in different regions i.e. shallow (L1, L4 and L6) or deep water (L2 and L5), influenced by fluvial SPM (L1 and L4) or by cliffs erosion (L3).

Time series of shear stress velocity at locations L1, L2, L3, L4, L5 and L6 (Fig. 5d, h, l and Fig. 6d, h, l) capture the periods of the spring and neap tide cycles (two cycles in a month in the North Sea). The

Table 2: Model grid points used to analyze annual time series of SPM, their locations, depths, annual mean shear stress velocity (V^*_{mean}), initial content of fine sediment in the seabed (f_{fine}) and SPM concentrations in the surface layer and in the bottom model layer (annual mean and range).

Location	Geographical position	Depth, m	V^*_{mean}, cm s^{-1}	f_{fine}, %	Surface SPM, mg l^{-1}	Near seabed SPM, mg l^{-1}
					mean and range	mean and range
L1	54.15°N, 07.98°E	39	0.91	43.62	13.92 (0.32 – 48.97)	25.79 (0.77 – 63.25)
L2	54.55°N, 00.65°E	61	0.59	2.44	0.16 (0.01 – 0.49)	3.95 (0.11 – 15.69)
L3	53.07°N, 01.98°E	35	1.60	0.83	1.21 (0.08 – 8.49)	25.21 (0.39 – 51.40)
L4	53.07°N, 04.27°E	32	0.89	0.73	1.04 (0.03 – 10.52)	6.80 (0.32 – 36.57)
L5	54.07°N, 02.81°E	60	0.98	10.30	0.04 (3e-4 – 2.86)	1.75 (0.16 – 47.18)
L6	55.45°N, 02.81°E	36	0.76	2.26	0.03 (1e-4 – 1.26)	0.06 (4e-4 – 8.38)

vertical mixing in these points, especially in L2 and L5 was not strong enough to redistribute SPM from the bottom water layer to the surface producing large difference (up to 40 mg l^{-1}) between SPM concentration at the surface and near seabed. Despite the similar depth, SPM concentrations in the bottom water layer at locations L2 and L5 are quite different (0.11 – 15.69 mg l^{-1} and 0.16 – 47.18 mg l^{-1} respectively) even during the stormy period from January through March characterized by the wind speed of $>$ 20 m s^{-1} and significant wave height of up to 6 m (Fig. 5f, g and Fig. 6f, g). This difference is attributed to the lower content of fine sediment in the seabed at L2 compared to L5 (Table 2). Stormy conditions at the end of January lead to a small increase in the surface SPM concentration at L5 (from near 0 to about 3 mg l^{-1}) and at L2 (up to 0.5 mg l^{-1}). The annual mean shear stress velocity (V^*_{mean}) was 0.59 cm s^{-1} at L2 and 0.98 cm s^{-1} at L5. As a result, SPM concentration increases in these two locations are caused primarily by resuspension (threshold value for resuspension V^*_{res} is 1.0 cm s^{-1}) rather than erosion (threshold 2.8 cm s^{-1} which is rarely exceeded). In contrast to concentrations of SPM in the bottom water layer, the surface SPM concentrations at these two relatively deep locations are very close in magnitude (around 0.5 – 2.5 mg l^{-1}, see Fig. 5e and Fig. 6e; Table 2) because the influence of waves on the vertical mixing can not reach seabed.

The circulation patterns in the North Sea with high current velocities in shallow and coastal regions lead to the formation of zones with very low fine sediment content in the seabed, for example near English cliffs at location L3 (Fig. 5i). High shear stress velocities at L3 (up to 1.6 cm s^{-1}) mainly generated by currents, often exceed the threshold value for erosion (Fig. 5l) making sedimentation hardly possible. Such conditions lead to washout of fine sediment near cliffs and keep the eroded and advected SPM in suspension, resulting in the high annual mean SPM concentration ($>$ 25 mg l^{-1}) in the near-bottom layer.

In shallow regions of the North Sea, currents and waves may become equally important and may result in a strong vertical mixing. Although points L1 and L4 are located in shallow regions, there are vertical gradients in the mean annual SPM concentrations (Fig. 5a and 6a), with the concentrations of 13.9 mg l^{-1} at the surface and 25.8 mg l^{-1} in the bottom layer in L1 and 1.0 mg l^{-1} at the surface and 6.8 mg l^{-1} in the bottom layer at L4. Different concentrations of SPM in these locations are explained by the much higher fine sediment content of 43.6 % in the seabed at L1 compared to only 0.73 % in L4 (see Table 2). During calm periods (April-October), the contribution of currents on V^* in these locations is dominant and the wave components are not essential. Under such conditions the turbulent diffusion is not strong enough to redistribute the SPM homogeneously in the water column so that the strong vertical surface-seabed gradient is formed. The difference of SPM concentrations between the surface and the near bottom water layer is high, up to 50 mg l^{-1} in L1 and up to 35 mg l^{-1} in L4. SPM concentration in the bottom water layer correlates well with the shear stress velocity (correlation coefficient of up to 0.85) in L1 during the calm period from 20.09.02 to 03.10.02.

The shear stress velocity continually exceeded the threshold value for resuspension in L1 and L4 (Fig. 5d and 6d) thereby the water column is burdened with SPM. Additional wave forcing during stormy periods in January-March and October-November with the wind speed of $>$ 12 m s^{-1} and H_s of up to 5 m (Fig.

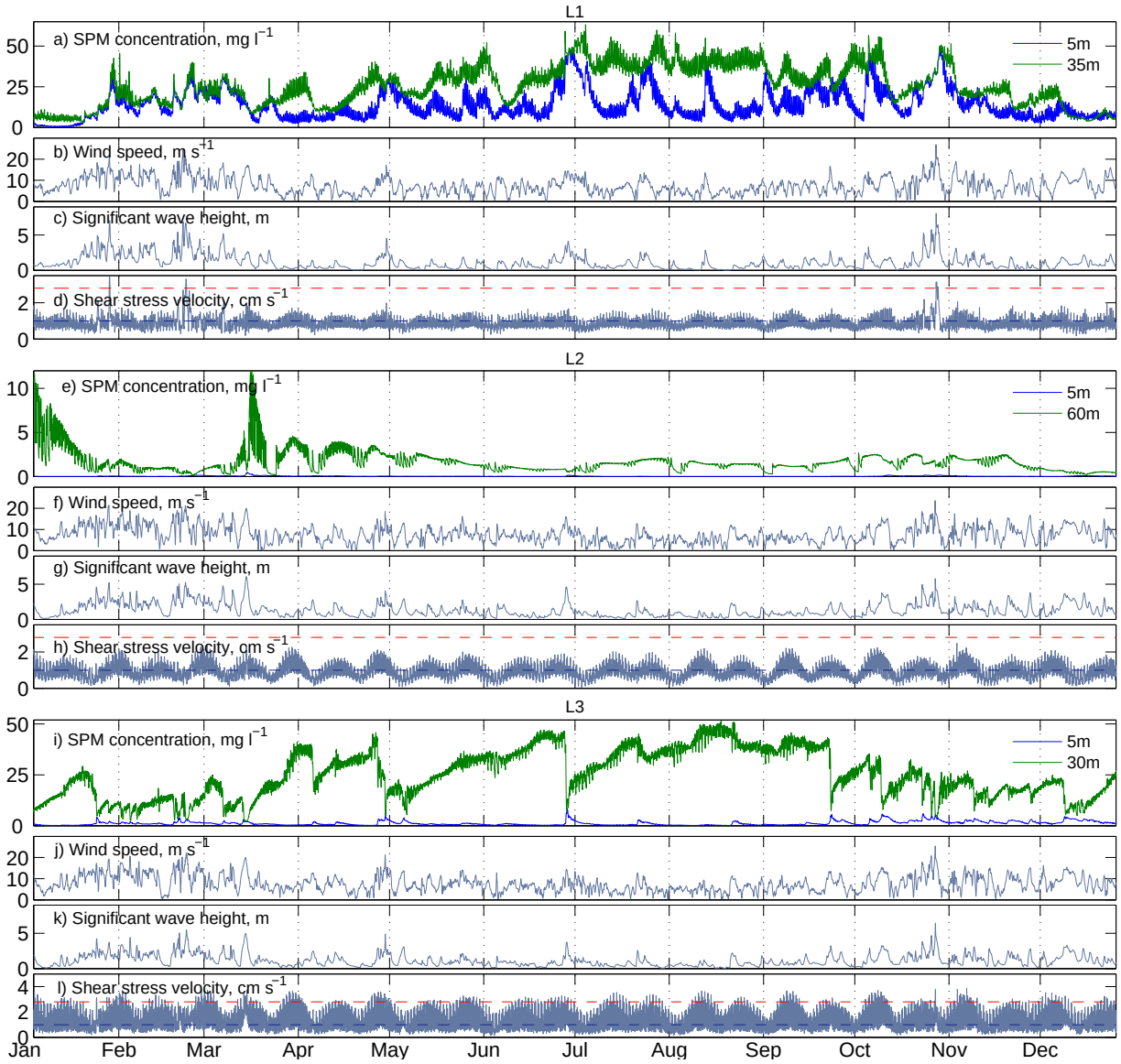

Figure 5: Calculated time series of SPM concentrations (mg l^{-1}) in the North Sea in 2002 at locations a) L1, e) L2 and i) L3 in the surface layer (blue line) and in the near bottom water layer (green line), and corresponding wind speed (m s^{-1}; b, f and j), significant wave height (m; c, g and k) and shear stress velocities (cm s^{-1}; d, h and l) with threshold values V^*_{res} (yellow dashed line) and V^*_{ero} (red dash line).

5b and 5c and Fig. 6b and 6c) results in strong vertical mixing of SPM. During January, February and October, the values of V^* sometimes exceeded V^*_{ero} . Consequently, after the first erosion event at the end of January the SPM concentrations increased from 8 to 25 mg l^{-1} at L1 and reached 2 mg l^{-1} in the surface and in the bottom water layers at L4 (Fig. 5d and 6d). Currents and waves were again strong enough to result in the shear stress which exceeds V^*_{res} also in February and March.

The next erosion event at the end of February did not play a significant role in changing the SPM concentrations because the mass eroded in January was still in suspension and the content of fine sediment in the seabed was low. Another erosion event occurred at the end of October in both locations. At L1 erosion and strong vertical mixing formed high SPM concentrations (up to 45 mg l^{-1}) in the whole water

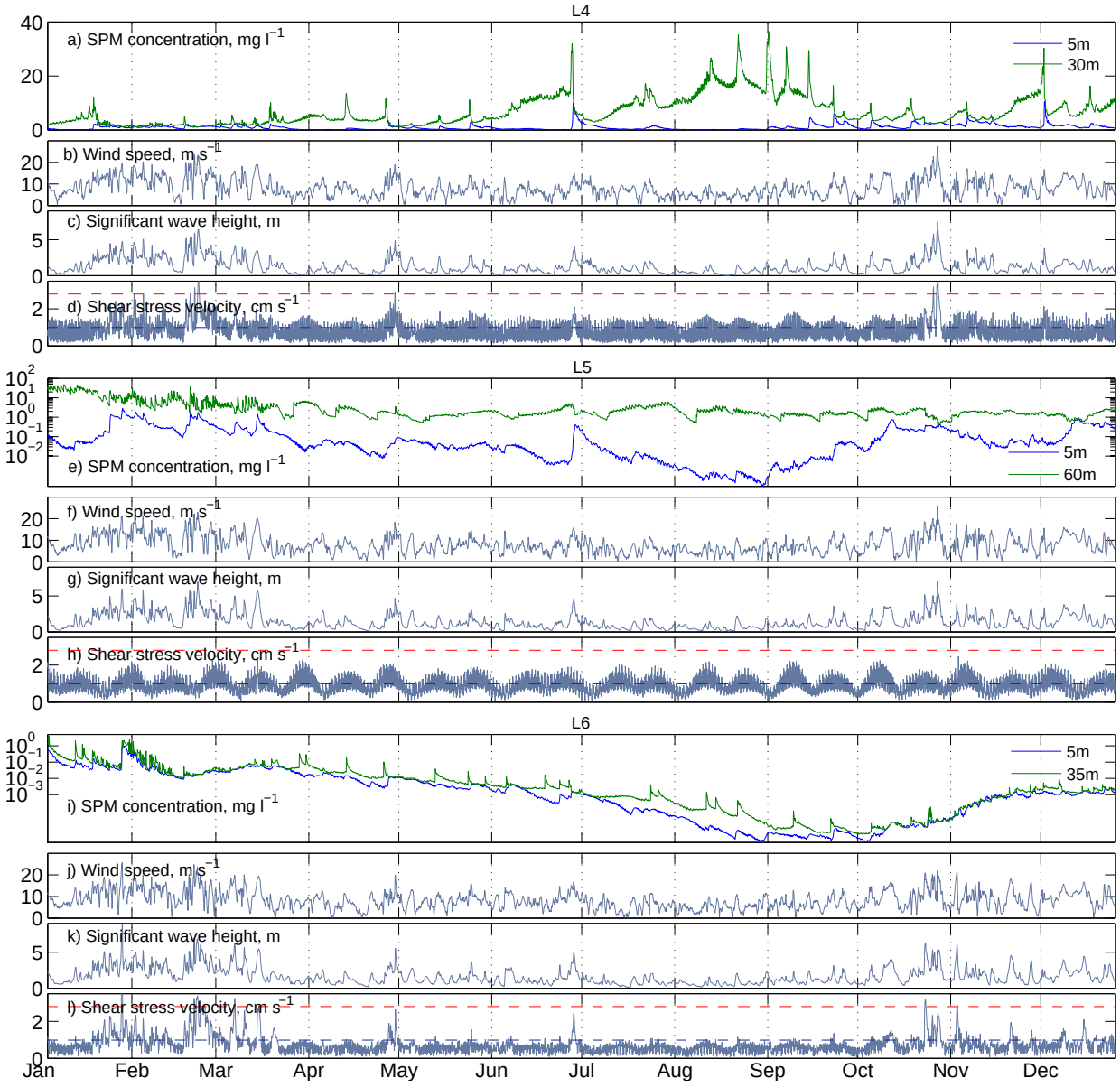

Figure 6: Calculated time series of SPM concentrations (mg l^{-1}) in the North Sea in 2002 at locations a) L4, e) L5 and i) L6 in the surface layer (blue line) and in the near bottom water layer (green line), and corresponding wind speed (m s^{-1}; b, f and j), significant wave height (m; c, g and k) and shear stress velocities (cm s^{-1}; d, h and l) with threshold values V^*_{res} (yellow dashed line) and V^*_{ero} (red dash line).

column. At L4 the change of SPM concentrations due to erosion is not so dramatic because of the lower content of fine sediment in the seabed.

Under calm conditions later in the year, sinking and sedimentation lead to the formation of large vertical gradients in the SPM concentration in L1 and L4. The maximum of the SPM concentrations in the bottom water layer occurs at the end of June (60 mg l^{-1}) in location L1 and in September (38 mg l^{-1}) in L4. The pronounced peaks in the surface SPM concentration in July in L1 (50 mg l^{-1}) and in June in L4 (8 mg l^{-1}) are shaped by the advection of additional SPM mass from neighboring grid points and resuspension.

An increase in the significant wave height in L4 at the end of June and later, at the end of August and

during the first half of September leads to an increase of the shear stress velocity and SPM concentration. This increase occurs only in the bottom layer (Fig. 6a) because additional wave mixing was not strong enough to redistribute SPM from the bottom to the surface.

Because of the relatively low fine sediment content in the seabed (2.26 %, Table 2) and low mean shear stress velocity (0.76 cm s^{-1}, Table 2) in the open North Sea at location L6, the surface SPM concentrations (Fig. 6i) remain low throughout the simulation period (<0.03 mg l^{-1}) despite erosion events and strong vertical mixing during storms in January-February and October-November characterized by the wind speed of up to 20 m s^{-1} and H_s of up to 8 m (Fig. 6j and k). During other months in 2002, the values of shear stress velocity in this location were generally below V^*_{res} (Fig. 6l) and did not cause significant increase in the SPM water concentration. Annual mean SPM concentration was 0.03 mg l^{-1} at the surface and 0.06 mg l^{-1} in the near bottom layer. The second erosion event in L6 in October was not intensive enough to increase the SPM concentration in the bottom water layer of the model. In comparison to the first erosion event at the end of January, the shear stress velocity in October was smaller (3.2 cm s^{-1} in October and 5.6 cm s^{-1} in January) and not high enough to erode new sediment from deeper bottom layers.

4. Vertical SPM dynamics in the water column and in the seabed

Vertical distributions of SPM in the North Sea vary from full mixing over the entire water column to strong stratified structure with large vertical gradients in SPM concentrations. Thus, we chosen a vertical section along 3°E (Fig. 2) for the vertical SPM distribution analysis as it includes circulation patterns for different regions of the North Sea, such as off-shore, coastal, close to estuaries, and in the passage of water entering from the English Channel. The vertical sections in water and in the seabed show two different distributions (see Sec. 5.3) of fine sediment during a storm on 28 January and calm conditions on 10 July 2002 (Fig. 7) with the typical for the calm and the storm periods values of wind speed and significant wave height (Fig. 7a and e). Calm conditions in July were characterized by the mean wind speed of 7.0 m s^{-1} and significant wave height of 0.8 m. During a storm on 28th of January the mean value of wind speed reached 22.5 m s^{-1} and significant wave height reached 6.7 m .

Due to frequent storms during winter accompanied by high waves (up to 10 m, Fig. 7a), the shear stress velocity (V^*) often exceeded the threshold values of resuspension and erosion, e.g. the mean value of V^* along the vertical section is 3.1 cm s^{-1} in January (Fig. 7d). During stormy conditions in January 2002, shear stress velocity exceeded the erosion threshold ($V^* > V^*_{ero}$; Fig. 7d) almost along half the section. The wave component (V^*_{wave}) dominated the shear stress velocity everywhere with the exception of the region near the English Channel, where the shear stress component due to currents (V^*_{cur}) was higher. Erosion events which occur on a time scale of minutes corresponding to the wave propagation time scale remove fine sediment from the seabed down to the erosion depth of up to 9 mm in the Dogger Bank (around 55°N; Fig. 7c). Note that according to model simulation, the seasonal maximum of erosion depth vary in 2002 and 2003 from 2.02 mm during calm period to 6.27 mm during storm period (e.g. Fig 7c and g and Table 3). High SPM concentrations (20-25 mg l^{-1}; Fig. 7b) are found near areas with hight fine sediment content in the seabed. Vertical mixing redistributes the SPM from lower to upper layers with the surface SPM concentrations > 15 mg l^{-1}.

When turbulence is not strong enough to keep particles in suspension, they settle to the bottom. In summer, the model calculations show relatively high SPM mass in the uppermost seabed layer (Fig. 7g). SPM accumulated in seawater during storm periods sinks to the bottom model layer and deposits into the seabed (Fig. 7f and g). The shear stress velocities are generally below the resuspension threshold with the mean value of V^* along the section of 0.8 cm s^{-1}. In the calm periods, the contribution of V^*_{wave} is small (Fig. 7h) and resuspension occurs only near the English Channel (51.4° – 52.3°N) due to higher currents velocities in this area. Despite resuspension events, the SPM concentration at the sea surface is low (about 1-2 mg l^{-1}; Fig. 7f) because the content of sediment in the seabed is also low (<0.1 kg m^{-2}; Fig. 7g) and additional wave forcing with the wave height of about 1 m is not strong enough to redistribute SPM in the water column (Fig. 7e).

Generally, sedimentation occurs in the deeper areas of the North Sea (>30 m). Exchange processes between the bottom water layer and the upper seabed layers are slow during the calm period. This enables

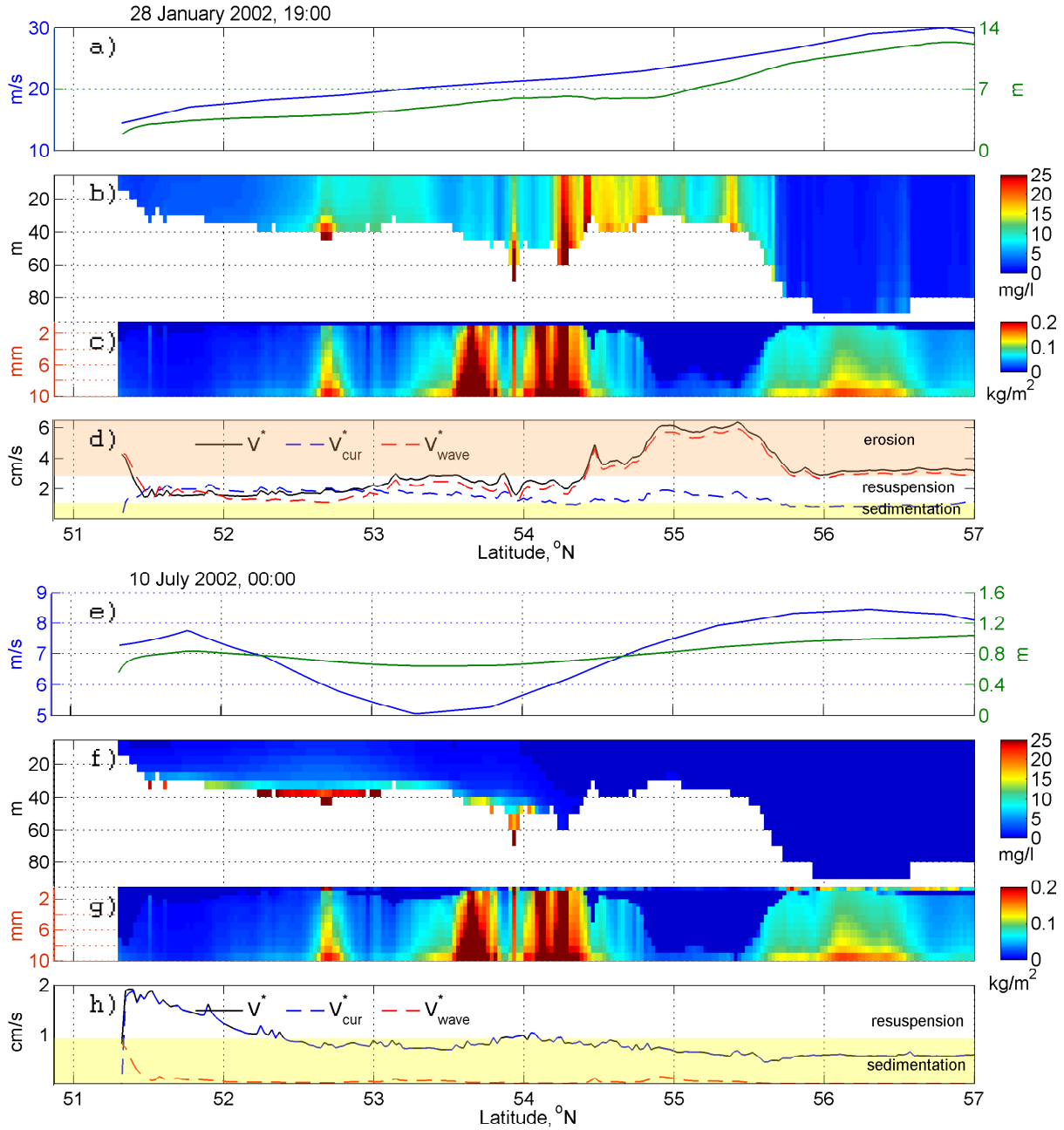

Figure 7: Vertical sections of modeled SPM concentration (mg l^{-1}) from South to North along 3°E in the water b) and f), sediment mass (kg m^{-2}) in the upper 10 mm of the seabed c) and g) on 28 January and on 10 July 2002 and corresponding shear stress velocity V^* (m s^{-1}) d) and h) with its components due to waves (red) and currents (blue); threshold values of V^* for erosion, resuspension and sedimentation are indicated by colored areas. Correspond wind speed (m s^{-1}) a) and e) (blue) and significant wave height (green) are shown.

the horizontal advection to redistribute SPM forming zones of high SPM concentrations in the bottom water layers (20-25 mg l^{-1}; Fig. 7f). Sedimentation process adds fine sediment mass in the uppermost seabed layer (Fig. 7g), which then redistributes slowly to the deep layers in the seabed due to bioturbation.

5. Seasonal dynamics of SPM and its forcing factors

Based on the analysis of meteorological and waves conditions in the North Sea, we distinguished two periods with different SPM distribution patterns further named as the *calm* period typically occurring during the warm season (from 15 April to 15 October) and the *storm* period common for the cold season (from 15 October to 15 April). Relative contribution of currents and waves into the shear stress velocity is different during these periods. Accordingly, they have a different impact on the SPM exchange processes at the seawater-seabed interface and on the vertical mixing of SPM in the water column.

5.1. Seasonal variations of currents and waves

As mentioned in Section 2.1.2 and Section 2.1.3, currents and waves are two equally important factors that force the dynamics of SPM in the North Sea. They influence the turbulence intensity and vertical mixing in the water column and the shear stress in the near-seabed water layer, which drives the seabed-water SPM exchange processes (Section 2.1.3). The mean seasonal values of significant wave height and the maximum seasonal currents velocity can be used to detect areas in the North Sea with potentially high shear stress velocities that are prone to erosion and resuspension events.

The typically cyclonic general circulation pattern in the North Sea (Lenhart and Pohlmann, 1997; Schrum, 2001) is mainly formed due to the Atlantic and the English Channel inflow. During the predominant lunar M2-tide cycles (Bartels, 1957) the tidal component of the currents prevails over the whole currents system. Therefore the currents velocity distribution in the North Sea does not differ significantly during calm and storm periods and between the years 2002 and 2003 (Fig. 8). This leads to permanently strong influence of currents on the shear stress velocity in the shallow regions such as the German Bight, along the British coast and in the English Channel. As shown in the following section (see Section 5.2, Fig 10c and d), the currents component of the shear stress velocity alone can be sufficiently high to cause resuspension during both the calm and the storm periods. In other regions (e.g. Dogger Bank and German Bight) the maximum surface currents velocity increases from 60 cm s^{-1} to 100 cm s^{-1} due to higher wind speed during the storm period.

In contrast to currents, significant wave height (H_s) has pronounced seasonality in the North Sea. The values of H_s during storm period can be up to 1.5 m higher than during calm period in 2002 and 2003 (Fig. 9). The highest seasonally averaged H_s during the calm period was 1.29 m in 2002 and 1.03 m in 2003 (Fig. 9a and c). During the storm period, the highest of seasonally averaged H_s was 2.54 m in 2002 and 2.21 m in 2003 (Fig. 9b and d).

Although the seasonally averaged H_s (2.54 m) during the storm period in 2002 was higher than in 2003, the mean H_s during the calm period in 2003 (1.03 m) exceeded its mean in 2002 (0.99 m). Potentially it increases the frequency of resuspension events adding fine sediment mass in the water and can lead to higher surface SPM concentrations during calm period in the year 2003. The mean H_s during the storm period in 2002 (1.86 m) exceeds its mean in 2003 (1.64 m), but higher mean H_s during the calm period in 2003 indicates more intensive resuspension and vertical mixing with more suspended fine sediment in the water column and therefore leads to higher surface SPM concentration in 2003 during storm period, even with smaller maximum value of the seasonally averaged H_s.

The highest values of H_s during both periods were in the open North Sea because of the combination of topography with predominant wind direction and the storms coming from the North Atlantic. The influence of the storm events during the storm period can be illustrated by the position of the 1.5 m isoline of the seasonal mean significant wave height (H_s), which is located in the open North Sea during the calm period, and very close to the coast during the storm period (see Fig. 9).

In the shallow regions (depth about 40 m or less), such as the Dogger Bank, the topography effect (such as dissipation of waves due to interaction with the seabed) on the H_s is pronounced even during calm period (Fig. 9a and b). It is more intensive during the storm period (Fig. 9c and d) because of the higher values of H_s. The role of the wave component of the shear stress velocity in the SPM exchange processes at the water-seabed interface is significant in the shallow regions during both the calm and the storm periods. Therefore, concentrations of SPM in these areas can be very high (> 50 mg l^{-1}) during stormy weather.

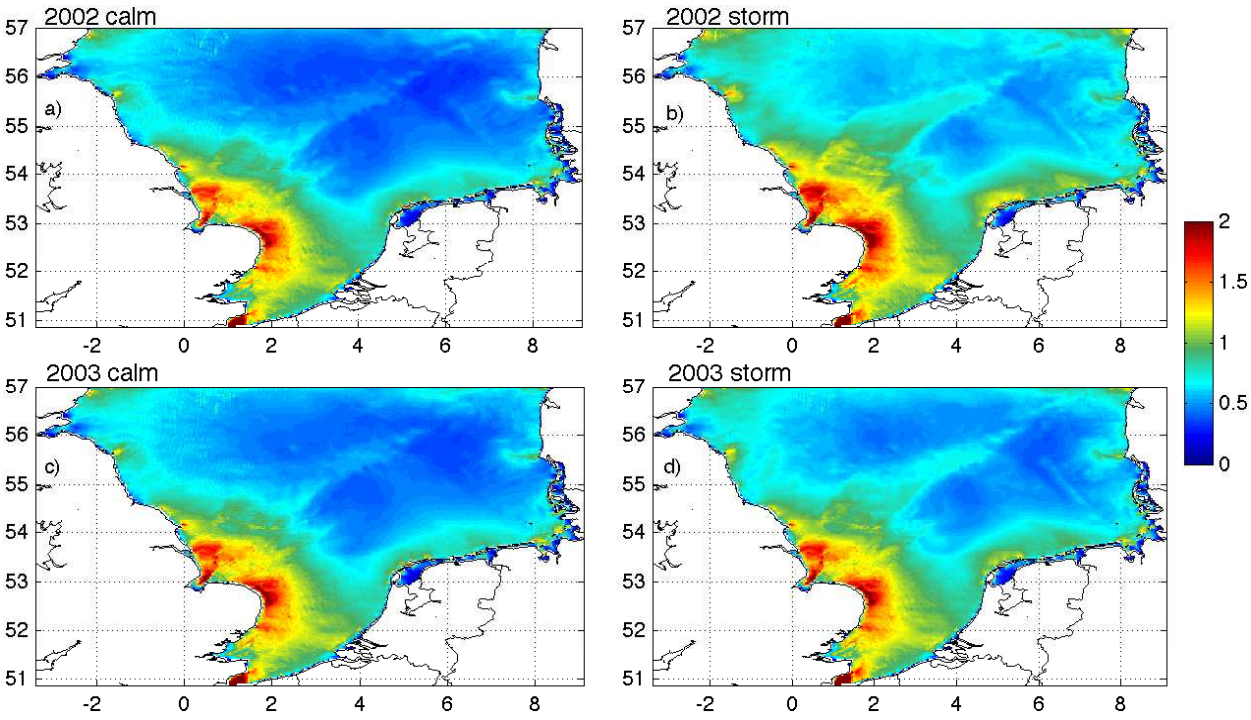

Figure 8: Seasonal maximum of surface current velocity (m s^{-1}) calculated by the model: a) and c) for the calm (15 April – 15 October) and b) and d) for the storm (15 October – 15 April) periods for the year 2002 and 2003.

5.2. Seasonal variations of shear stress velocity and SPM exchange processes

Seasonal variations of the shear stress velocity (V^*) in the years 2002 and 2003 for the entire model domain and its shallow part (depth < 40 m) are summarized in Table 3. Mean values of V^* in 2003 (0.846 cm s^{-1}) is close to the value in 2002 (0.849 cm s^{-1}). However, as in case with waves (see 5.1), the maximum V^* (5.695 cm s^{-1}) was higher in 2002 compared to 2003 (5.520 cm s^{-1}). The mean value of V^* during the calm period in 2003 (0.766 cm s^{-1}) was higher in comparison to 2002 (0.758 cm s^{-1}). This means that less SPM was deposited on the bottom during the calm period in 2003 and more fine sediment remained in suspension in the water column.

Table 3: Shear stress velocities V^* (cm s^{-1}) and erosion depth h_{ero}(mm) in the North Sea in the years 2002 and 2003 during a calm (15 April – 15 October) and storm (15 October – 15 April) periods.

	2002		mean	2003		mean
	calm	storm		calm	storm	
Entire model domain						
V^* mean	0.758	0.940	0.849	0.766	0.926	0.846
V^* max	5.566	5.695	5.695	5.520	5.521	5.520
h_{ero} mean	0.006	0.03	0.018	0.003	0.014	0.009
h_{ero} max	5.75	6.27	-	2.02	2.08	-
Part of model domain with depth < 40 m						
V^* mean	0.97	1.24	1.11	0.98	1.22	1.10

The seasonal mean stress velocity (Table 3 and Fig. 10a and b) allows to identify different zones in the southern North Sea where one or another seabed-water exchange process prevails. We show the influence of waves on the shear stress near seabed in the year 2002 as it was characterized by higher value of significant wave height (Fig. 9).

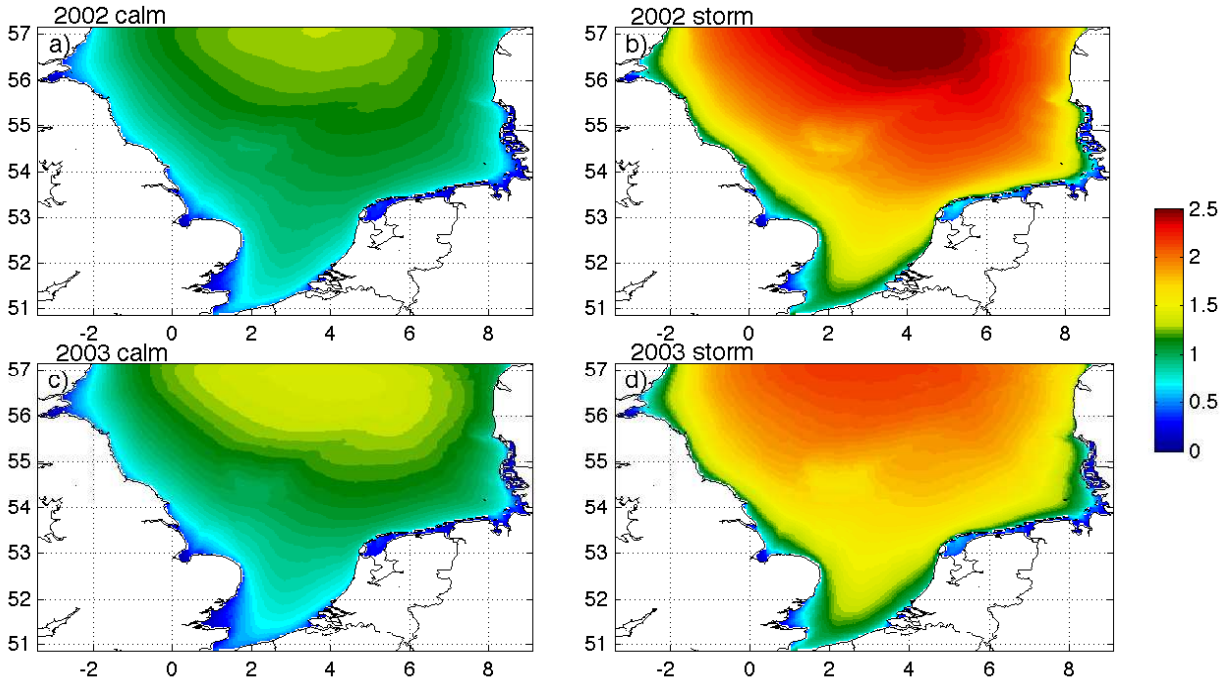

Figure 9: Seasonal mean significant wave height (m) calculated by the WAM model: a) and c) for the calm (15 April – 15 October) and b) and d) for the storm (15 October – 15 April) periods for the year 2002 and 2003.

In line with the general circulation pattern, the currents component of V^* (Fig. 10c and d) does not differ significantly during the calm and the storm periods. It shows permanent resuspension zones in the south-western part of the North Sea, along the Netherlands coast and in the German Bight. Such pattern explains the occurrence of the high surface SPM concentrations in these areas even under calm conditions throughout the whole year.

The effect of waves on the SPM distribution is irregular. Nevertheless, it plays a dominant role during storm periods, when the distribution of V^* changes under the influence of the wave component. With the increasing frequency of storm events in the North Sea, new resuspension zones occur (Fig. 10f). The location of these zones is mainly determined by the topography. The energy of the waves coming from the North Atlantic dissipates mainly in the shallow regions, such as the Dogger Bank and the German Bight. This energy results in the increase of V^* , to values high enough for resuspension. Generally, the resuspension zone during the storm period covers the southern part of the model area, shallow areas in the open North Sea and most of the German Bight.

The increase in the V^* leads to erosion, but the seasonal mean V^* distributions do not show permanent erosion zones, because erosion events have a short duration and are rare (as shown in Section 3). The erosion zones occur when V^* exceeds the threshold value V^*_{ero} . They are located in the regions with a combination of high V^*_{cur} and V^*_{wave} (Fig. 10).

Sedimentation zones in the North Sea are located mainly in the deep areas, where the currents- and waves-induced shear stress in the near-seabed layer is not high enough to keep SPM in suspension. The sedimentation zones cover the open part of the model area, excluding the Dogger Bank region during the storm period. In contrast to erosion, seasonal mean values of V^* clearly define sedimentation zones, because hydrodynamic conditions in the deep North Sea do not differ significantly during calm and storm periods in the near seabed water layers.

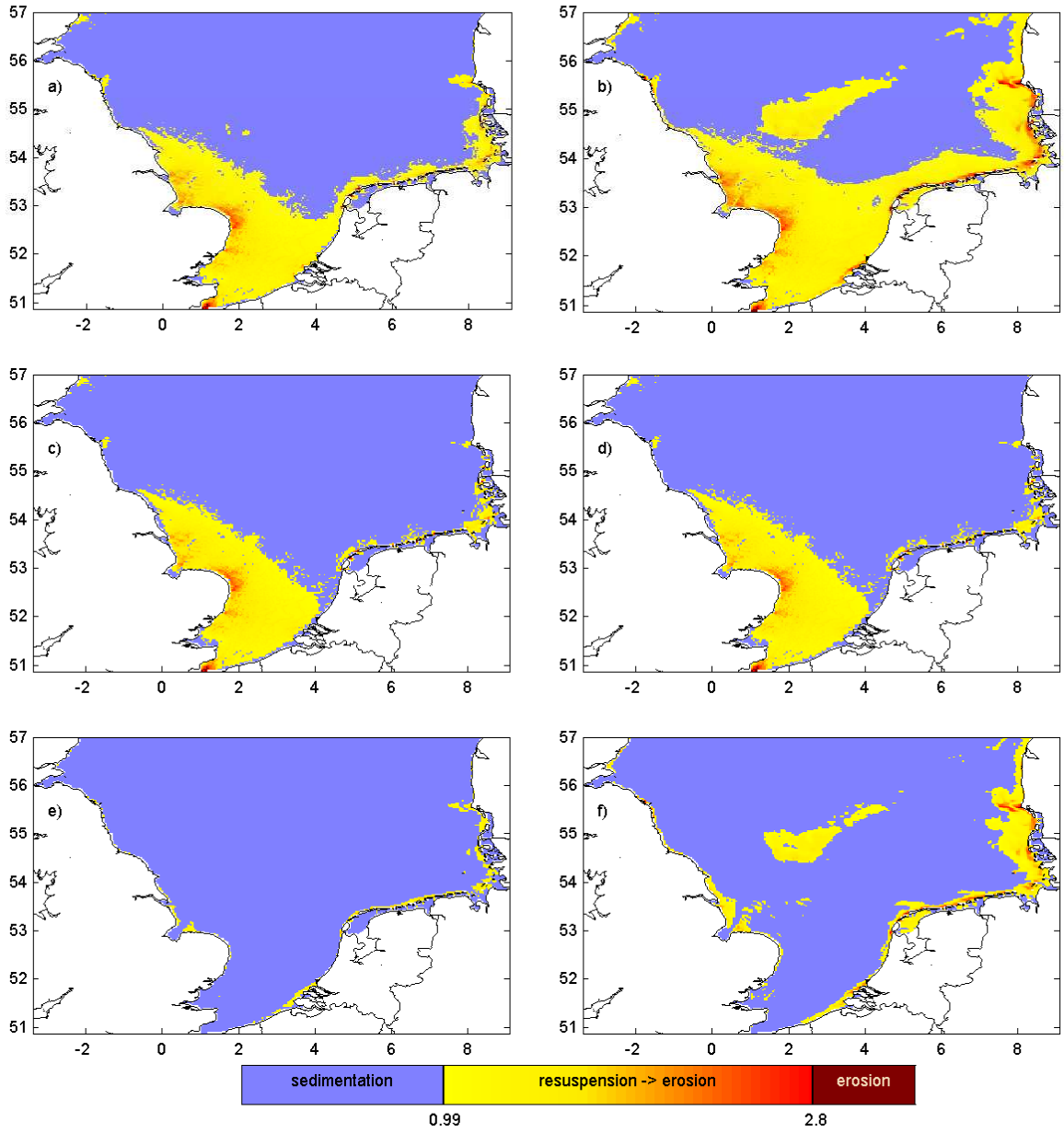

Figure 10: Seasonal mean shear stress velocity (a, b) and its components due to currents (c, d) and waves (e, f) during calm (left column) and storm (right column) periods in the year 2002.

5.3. Seasonal variations of the surface SPM concentrations

We illustrate seasonal variations of the surface SPM by comparing its distribution during the storm and the calm periods. The difference in these two SPM distributions is explained by more intensive fine sediment exchange processes between the seabed and seawater and more intensive vertical mixing due to waves during storm periods. The seasonality in the distribution of SPM may be expressed not only by a deviation from the mean surface SPM concentration (see Table 4), but also by the portion of the model area in which the surface SPM concentration exceeds the mean modeled SPM concentration in the years 2002 and 2003 (3.0 mg l^{-1}). This exceeding is more pronounced in the shallow areas of model domain with a depth of 40 m or

less (see Table 4). Such calculation indicates that in 2002, SPM concentrations at the surface were above the mean value in 6% (12% in shallow areas with a depth < 40 m) of the model domain during the calm period and in 9% (18.9%) during the storm period. Accordingly, in 2003, 11.5% (21.4%) of the model domain had SPM concentrations above average in the calm period and 38.5% (62.5%) in the storm period respectively. Mean significant wave height and mean shear stress velocity during the calm period in 2003 were higher than

Table 4: Surface SPM concentration (mg l^{-1}) in the North Sea in the years 2002 and 2003 during a calm (15 April – 15 October) and storm (15 October – 15 April) periods.

	2002		mean	2003		mean
	calm	storm		calm	storm	
Entire model domain						
mean	1.98	2.01	2.00	2.74	5.22	3.98
min	1e-3	0.01	0.01	5e-4	0.01	0.01
max	582	558	570	335	329	332
% coverage by > 3 mg l^{-1}	6.0	9.0	7.5	11.5	38.5	25.0
Part of model domain with depth < 40 m						
% coverage by > 3 mg l^{-1}	12.0	18.9	15.5	21.4	62.5	42.0

in 2002 (Table 3) so that the enhanced vertical mixing kept more fine sediment in the water column in 2003. This explains higher mean SPM concentrations in 2003 (3.98 mg l^{-1}) compared to 2002 (2.00 mg l^{-1}) all over the year. SPM plumes develop under both the storm and the calm conditions. Initial distribution of the

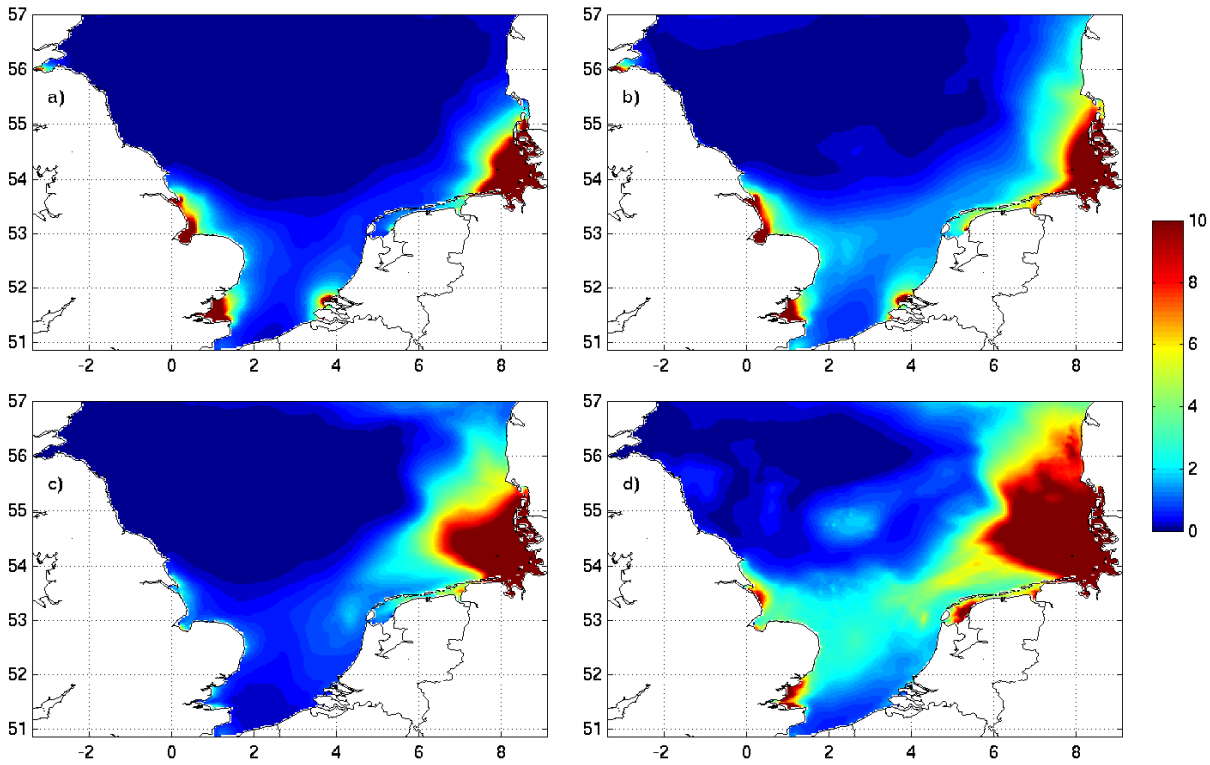

Figure 11: Seasonal mean modeled SPM concentrations (mg l^{-1}) in 2002 and 2003 averaged for the warm period (15 April – 15 October, a and c) and for the cold period (15 October – 15 April, b and d).

fine sediment in the bottom (Fig. 2) shows regions where high SPM concentrations at the surface potentially

occur. Under calm conditions, transport with sea currents determines the location of zones with permanent high horizontal gradients of SPM concentration (SPM fronts) near the coast, close to river mouths and near the English cliffs (Fig. 11a). The seabed-water exchange processes are always intensive in the shallow German Bight, also under calm conditions due to relatively strong currents (Fig. 10). At these depths (up to 25 m), even small perturbations caused by currents and waves result in resuspension and erosion and increase the SPM concentration in the bottom water layer. The vertical mixing is sufficiently strong to redistribute high SPM concentrations (> 10 mg l^{-1}) from the bottom to the sea surface. Additionally, the German Bight is supplied with SPM from the rivers, mostly from the river Elbe (Fig. 3). Note, that in 2003 the rivers influence on the surface SPM concentration is not significant, because of the low fresh water discharge and low SPM loads (Fig. 3). This also explains the lower maximum value of the surface SPM concentration close to the Elbe mouth in 2003 (332 mg l^{-1} in contrast to 570 mg l^{-1} in 2002).

Vertical mixing in the German Bight dominates over the horizontal advection of fluvial SPM, even close to the river mouths because SPM deposits quickly (also supported by an SPM dumping experiment Siegel et al. (2009)), thus maintaining visible fronts near the coast. These SPM fronts propagate northwards parallel to the coast following the commonly observed counter-clockwise general circulation pattern in the North Sea (e.g. Pohlmann and Puls (1994)).

Seasonality in the SPM distributions is more pronounced in the off-shore areas, where the influence of local effects such as the rivers inflow and cliffs erosion is low. During the storm period, strong water-seabed exchange and mixing of SPM in the water column result in the expansion of the relatively high SPM concentration zone further into the open North Sea (Fig. 11b). However, the highest surface SPM concentrations still remain near the coast.

6. Conclusions

We modeled the fine sediment dynamics in seawater and in the seabed using a combination of the circulation, SPM transport and waves models in 2002 and 2003 in the North Sea. Vertical and horizontal distributions of modeled SPM concentration are in good agreement with available in-situ and remote sensing data for the North Sea. Our results indicate that it is essential to use a coupled circulation and SPM transport model with realistic forcing data with a temporal resolution of < 1 hour and instant values of shear stress velocity in order to resolve SPM processes with different time scales, e.g. flash erosion events and long-term transport by currents. Utilization of the instant values of the shear stress velocity leads to more realistic representation of the exchange processes (increasing of number of resuspension and erosion events) at the water-seabed interface and to more convenient comparison between the snap-shot satellite measurements and model results.

Model results reveal two different patterns in the SPM dynamics emphasizing the different role of waves and currents in vertical distribution of SPM in the North Sea. One is observed under calm conditions, common for the warm period (15 April – 15 October), when SPM distribution is mainly shaped by the horizontal currents, which determine the location of an SPM front. Another pattern evolves instantly during storms and in the course of stormy periods (15 October – 15 April), when the vertical mixing due to waves during storm events dominates all other transport process and determines the vertical SPM concentration profile. Pronounced seasonality of SPM concentration is attributed to the seasonality of the shear stress velocity, which increases during the storm period as a result of waves and currents influence on the turbulence intensity. This phenomenon is especially visible in the shallow regions of the open North Sea (e.g. in the Dogger Bank). Model results show that the highest surface SPM concentrations during storm period was 120 mg l^{-1} in the open North Sea reaching up to 300 mg l^{-1} near the coast in the German Bight. In shallow regions close to the coast and river mouths, the SPM front occurs due to resuspension, erosion and vertical mixing. The contribution of fluvial SPM is relatively low (especially under calm conditions) because it deposits quickly close to the rivers estuaries.

The wave-induced component of the shear stress velocity dominates in the shallow regions during the entire storm period, excepting the regions with permanently strong currents (e.g. East Anglia coast). The seasonal mean shear stress velocity distribution allows to classify the southern North Sea in terms of different zones where one or another seabed-water exchange process dominates. The sedimentation zone is located

mainly in the open North Sea, the zones of resuspension occupy the shallow regions along the coast and in the open North Sea around the Dogger Bank. The zones where erosion occurs are located in the English Channel, along the UK east coast and in the German Bight. Individually or acting in concert, both currents and waves potentially lead to erosion in these areas of the North Sea.

7. Acknowledgments

This study is supported by the Helmholtz-EOS research network of the Helmholtz Association.

A. Shear stress velocity

Shear stress velocity is calculated from the shear stress τ and the actual water density ρ:

$$V^* = \sqrt{\tau/\rho} \tag{13}$$

The mean shear stress τ_{mean} (kg s^{-2} m^{-1}) is calculated based on its currents (τ_{cur}) and the wave (τ_{wave}) components following Soulsby (1997):

$$\tau_{mean} = \tau_{cur}\left[1 + 1.2\left(\frac{\tau_{wave}}{\tau_{cur} + \tau_{wave}}\right)^{3.2}\right] \tag{14}$$

The maximum value of the shear stress τ_{max} determines the threshold of motion with the angle between the currents and the wave direction ϕ:

$$\tau_{max} = \sqrt{\left(\tau_{mean} + \tau_{wave}\cos\phi\right)^2 + \left(\tau_{wave}\sin\phi\right)^2} \tag{15}$$

The currents component of the shear stress τ_{cur} is calculated from the quadratic friction law with the currents velocity in the lowest water layer U m s^{-1} and the friction coefficient C_D:

$$\tau_{cur} = \rho C_D U^2 \tag{16}$$

where C_D is defined as:

$$C_D = 0.16\left(1 + \ln\left(\frac{Z_0}{H_{kb}}\right)\right)^{-2} \tag{17}$$

where the roughness length in meters $Z_0 = d_{50}/12$ with the mean grain size $d_{50} = 0.00025$ (m) and H_{kb} (m) is the thickness of the lowest water layer.

The waves component of the shear stress τ_{wave} (kg s^{-2} m^{-1}) with the maximum of the horizontal orbital wave velocity U_w and the wave friction factor f_w is calculated as:

$$\tau_{wave} = 0.5\rho f_w U_w^2 \tag{18}$$

Assuming an equivalent sine wave for the significant wave height H_s, the peak period T, and the wave number k at a water depth h U_w is calculated as:

$$U_w = \frac{\pi H_s}{T\sin\left(kh\right)} \tag{19}$$

The wave friction factor f_w is determined by the maximum of the rough bed friction f_{wr} and the smooth bed friction f_{ws} coefficients:

$$f_{wr} = 0.237\left(\frac{A}{k_s}\right)^{-0.52}, f_{ws} = BR_w^{-N} \tag{20}$$

The parameter $k_s = 2.5d_{50}$ is the Nikuradse roughness length, related to the grain size for hydrodynamically rough flows. $A = U_w T/2\pi$ is the semi-orbital excursion. The parameters of the smooth bed friction factor

f_{ws} depend on whether the motion is laminar or turbulent, according to the Reynolds number R_w with the kinetic viscosity $\nu = 0.0000012$ (m^2 s^{-1}):

$$R_w = \frac{U_w A}{\nu} \tag{21}$$

Finally, the parameters B and N are defined as follows:

$$\begin{array}{lcll} \text{if } R_w \leq 5 \times 10^5 \textit{ (laminar)} & \Rightarrow & B = 2, & N = 0.5 \\ \text{if } R_w > 5 \times 10^5 \textit{ (turbulent)} & \Rightarrow & B = 0.0521, & N = 0.187 \end{array}$$

B. Bioturbation parameters

Diffusion coefficient for bioturbation Av_{bio} (Eq. 8) decreases from 100 cm^2 a^{-1} at the seabed surface to 20 cm^2 a^{-1} at 20 cm depth. Av_{bio}^{max} represents the highest possible bioactivity. It decreases linearly (Pohlmann and Puls, 1994) with depth in the seabed indicating that more bioactivity occurs in the upper seabed levels. The seasonal factor s_f depends on the month with the highest bioactivity in October (s_f = 0.99) and the lowest in April ($s_f = 0.54$) (Fig. 12c). Intensity of bioactivity in different regions of the model

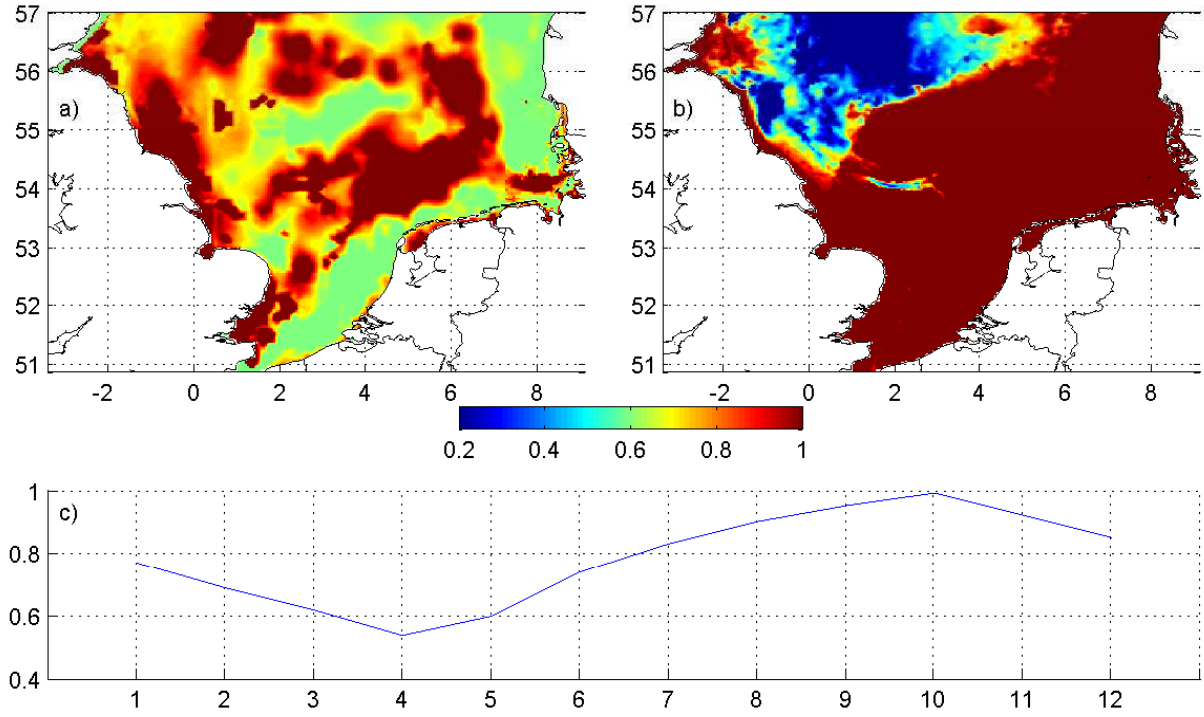

Figure 12: Bioturbation parameters: a) fine sediment content factor (l_f), b) depth factor (h_f) and c) seasonal factor (s_f).

area is described by two factors:
(a) l_f (range 0.6 – 1) (Fig. 12a) depends on the content of fine sediment in the seabed and
(b) h_f (range 0.2 – 1) (Fig. 12b) depends on the depth in the North Sea.
The product $s_f \cdot l_f \cdot h_f$ varies from 0.07 to 0.99. All factors are empirical and based on Puls (2006) and model test studies.

C. Correction of fine sediment map

The fine sediment map was corrected based on the MOS scene on 03.02.2000 captured a storm in the North Sea coming from the North Atlantic (28.01.2000-04.02.2000). According to the maximal wave height,

the storm peak occurred on 30.01.2000. Surface SPM concentrations calculated from the MOS scene after the storm peak were therefore smaller than the highest SPM concentrations possible under waves heights of about 10 to 12 m. In order to compensate this deficiency, an SPM model (Pleskachevsky et al., 2005) calculated the relative change of SPM concentration in the upper water model layer between the storm peak and the MOS scene. Model results showed that the average decrease of SPM mass after the storm peak was about 10% in the whole model domain (mainly due to sinking). This difference was added to MOS data in every grid point resulting in the SPM concentration during the storm peak determined backwards in time.

The contribution of erosion into SPM concentration during the storm was determined by subtracting the SPM concentration typical for the calm conditions in the North Sea (Doerffer and Fischer, 1994) from the SPM concentration calculated for the storm peak. Eroded SPM mass in seawater per unit area was estimated as the product of SPM concentration and depth assuming that under strong storm conditions SPM in shallow water areas (up to 40 m) is totally mixed and homogeneously distributed in the water column.

The seabed sediment map was corrected to attain the eroded SPM mass in water according to erosion depth (h_{ero}), obtained as a function of bottom shear stress velocity (see Eq. 6). For more details about the method used for processing of fine sediment map, see Pleskachevsky et al. (2005) and Gayer et al. (2006).

D. Comparison between modeled and in-situ SPM concentrations

Water samples were collected during several cruises in 2002 in the eastern and the south-eastern North Sea (Fig. 2). A direct comparison of model results with observational data was only possible for the data set 1 (Table 5), because sample processing allowed obtaining inorganic suspended matter (ISM) fraction separately from the total suspended matter (TSM) concentrations. The water samples were processed using gravimetric filter analysis of TSM (Strickland and Parsons, 1998; der Linde, 1998) and gravimetric filter analysis for ISM and organic suspended matter (OSM) (Hirota and Szyper, 1975). Generally, model results are in good agreement with the data set 1 (Table 5; Fig. 13) with a correlation coefficient of 78% and BIAS (Model-measurements) of 5.5 mg l^{-1}. The model captures the magnitude and spatial distribution of observed SPM concentrations.

Table 5: Summary of SPM in-situ data collected by GKSS Research Centre, German Federal Maritime and Hydrographic Agency (BSH) and Niedersächsisches Landesamt für Ökologie (NLOE) in the year 2002 used for the evaluation of model results (range and mean of measured and modeled SPM concentrations).

		Data set 1	Data set 2	Data set 3
Cruise organizer		GKSS	BSH	NLOE
Months of sampling		4,5	1, 2, 8, 9	3,11
Number of stations		46	105	34
Depths range		$1-36$ m	$8-12$ m	0.5 m
Parameter		ISM	TSM	TSM
Measurements, mg l^{-1}	range	0.00-20.40	0.44-243.86	20.00-140.00
	mean	2.07	7.88	63.21
Model range, mg l^{-1}	range	0.02-40.27	0.03-240.35	10.44-74.74
	mean	7.91	19.20	29.86

The TSM concentrations in data set 2 and data set 3 were measured without separating the organic and inorganic fractions (Table 5; Fig. 14). Depending on the season and location organic suspended (OSM) fraction in the North Sea can vary from about 20% of the TSM concentration in January in the southern part of the North Sea up to 50% in June in the Skagerrak area (Eisma and Kalf, 1987). Model results correlates well with the data sets 2 and 3, because in the periods from January to March and from August to November when measurements were conducted, the concentration of OSM is relatively low (Moll, 1998).

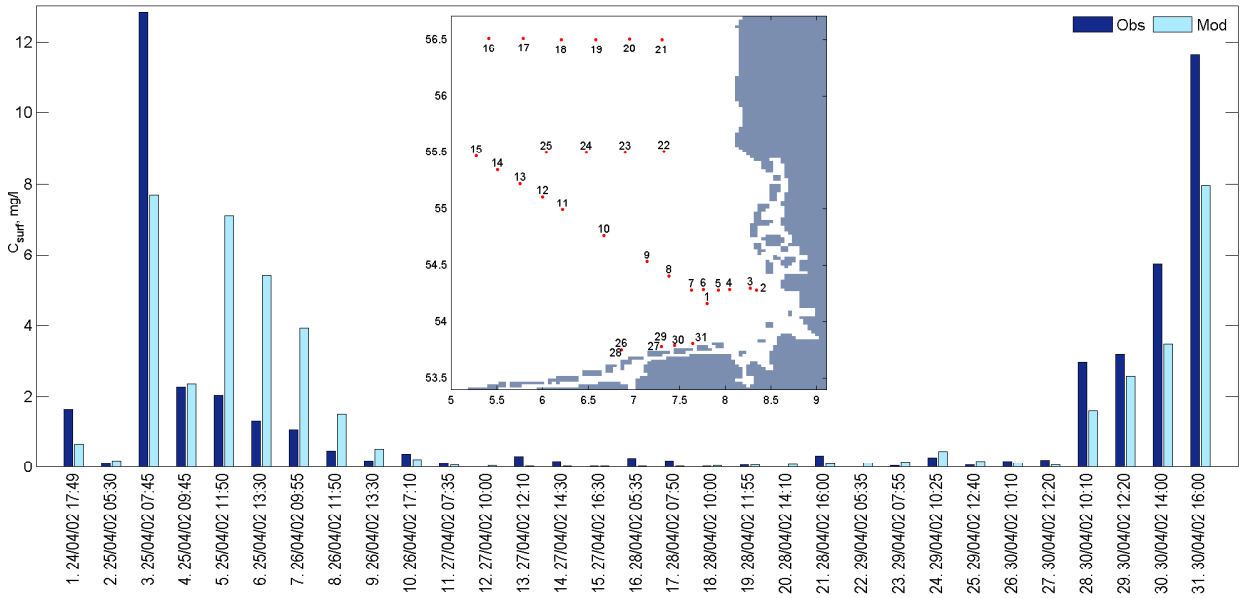

Figure 13: Measured and modeled surface SPM concentration (mg l^{-1}) in the North Sea at selected locations from the data set 1 (Table 5).

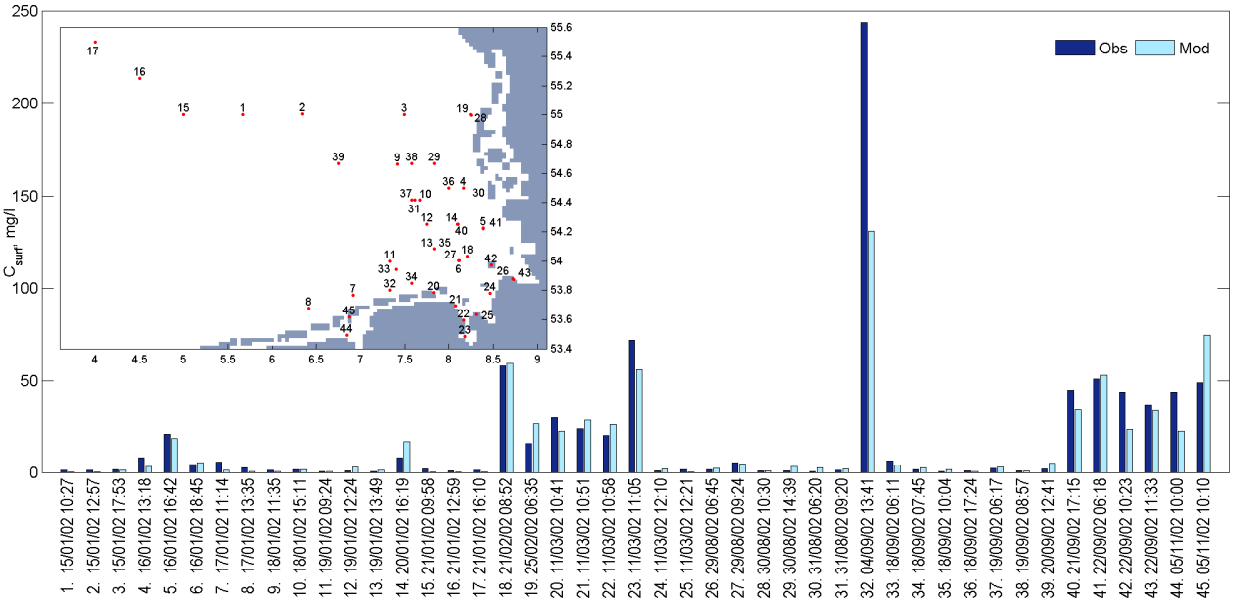

Figure 14: Measured and modeled surface SPM concentration (mg l^{-1}) in the North Sea at selected locations from the data set 2 and data set 3 (Table 5).

Data sets 2 and 3 include measurements from the very shallow locations (< 5 m). With the horizontal resolution of about 3 km and the vertical resolution of about 5 m the model is not capable to resolve SPM processes in very shallow coastal regions in details. Therefore, we selected only points with the minimum depth of 5 m which were located not closer than approximately 6 km (two model grid cells) away from the coast (Fig. 14). The correlation coefficient between measurements (data sets 2 and 3) and model results for these selected points is 92%, with a BIAS value of 3.1 mg l^{-1} (Fig. 14). The correlation coefficient for all

TSM measurements in the data sets 2 and 3 is lower (40%, BIAS = 3.9 mg l^{-1}).

We compared a few measured vertical SPM profiles from the data set 1 (Table 5) with model results (Fig. 15). Under calm conditions (when measurements were performed), SPM concentrations increase with depth with the maximum values in the bottom water layer. Such distribution, also captured in model results, is caused by the gravitational sinking and resuspension (Fig. 15; locations A, B and C). Measured SPM

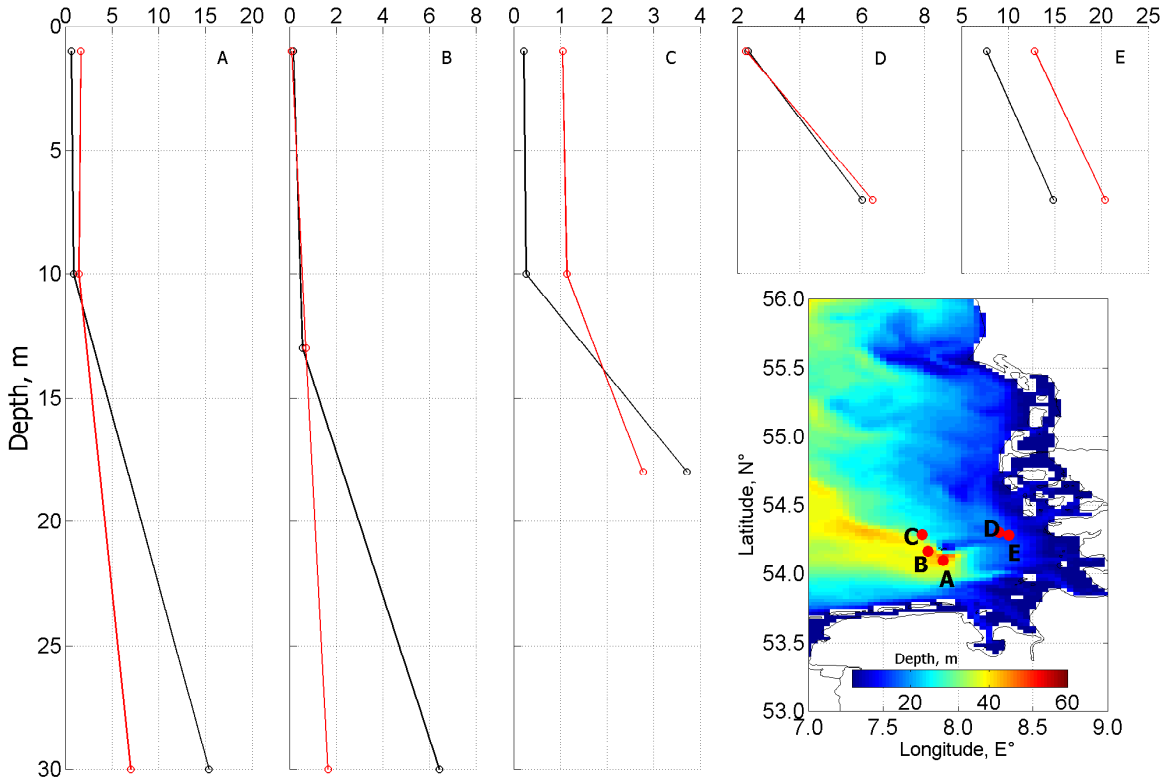

Figure 15: Observed (red; data set 1; Table 5) and modeled (black) SPM concentrations (mg l^{-1}) at locations A,B,C,D and E in the German Bight in April 2002.

concentrations range from 0.5 to 1.5 mg l^{-1} in the surface layer and from 3 to 15 mg l^{-1} in the lowest layer. Modeled SPM concentrations were up to 2.2 – 8 mg l^{-1} in the surface layer and up to 8 – 15 mg l^{-1} in the bottom water layer close to the coastal SPM front (see Section 5.3) and in the shallow regions, such as in the locations D and E (Fig. 15). One explanation for the overestimation of the modeled SPM concentrations in the bottom layer is the flocculation process, when fine particulates clump together into flakes, which is thought to be important but is not considered in this model configuration. When SPM concentrations are high, the flocculation increases the particle size and hence, the settling velocity according to Stokes' Law, laboratory experiments (Asaeda and Wolanski, 2002) and in-situ measurements (Dyer et al., 1996). Subsequently, it also increases the sedimentation rate (Section 2.1.3). As a result, more SPM will be removed from the bottom water layer.

E. Comparison between modeled and satellite SPM concentrations

Two types of satellite data obtained from MERIS (MEdium-spectral Resolution, Imaging Spectrometer operating in the solar reflective spectral range; Fig. 16) and MOS (Modular Optical Spectrometer; Fig.

17) are used for comparison with modeled surface SPM concentrations. SPM concentrations derived from MOS were produced by the German Aerospace Center (DLR, 2007). SPM concentrations form MERIS were calculated using the MERIS Case-2 Regional Processor (Doerfer et al., 2006).

MERIS scenes were selected so that they cover possibly the largest parts of the modeling domain (Fig. 16). Although the model captures general horizontal SPM pattern found in MERIS data, the SPM fronts in the satellite data are weaker compared to model results. SPM concentrations derived from satellite data have a cut-off maximum value ($\approx$ 70 mg l^{-1} for MERIS data), due to general constraints in the processing algorithms (Fettweis et al., 2007). Therefore satellite data may not be able to resolve larger gradients in zones with high SPM content, i.e. in the SPM fronts. MOS scenes were selected to show the SPM surface distributions during storm periods, e.g. in January 2002. MERIS data in this period is not available. Because storms are frequently accompanied by cloudy weather, these scenes (Fig. 17) only partially cover the model domain. MOS scene on 28 January 2002 (Fig. 17g) captures high surface SPM concentration in the German Bight induced by additional wave influence during the storm.

Modeled SPM concentration pattern at the surface resembles the seabed SPM distribution (cf. Fig. 16b, Fig. 17b and Fig. 2). SPM concentrations retrieved from satellite data (Fig. 16a and Fig. 17a) show the same horizontal distribution pattern. Modeled values are represented by the concentrations in the upper model layer (with the thickness of about 5 m). Satellite data is integrated over the signal penetration depth. The quantitative comparison between the modeled and satellite data is difficult due to the different definitions of the "surface" and because filtering of unrealistically high values of surface SPM concentration is needed. In contrast to SPM fields derived from satellite data, the modeled SPM surface distributions do not capture fine details in the horizontal patterns because of the numerical diffusion effect.

References

Asaeda, T. and Wolanski, E. (2002). Settling of muddy marine snow. *Wetlands Ecology and Management*, 10:283–287.

Backhaus, J. (1985). A three-dimensional model for the simulation of shelf sea dynamics. *Dtsch Hydrogr Z*, 38:167–187.

Backhaus, J. and Hainbucher, D. (1987). A finite difference general circulation model for shelf sea and its application to low frequency variability on the north european shelf. In Nihoul, J. and J, B. M., editors, *Three dimensional model of marine and estuarine dynamics*, Elsevier Oceanographic Series, pages 221–244. Elsevier.

Bartels, J. (1957). *Gezeitenkräfte, Handbuch der Physik*, volume II Band XLVIII. Geophysik.

de Swart, H. E. and Calvete, D. (2003). Non-linear response of shoreface-connected sand ridges to interventions. *Ocean Dynamics*, 53:270–277.

der Linde, D. V. (1998). Protocol for total suspended matter estimate. Technical report, JRC Technical Note.

DLR (2007). German aerospace center, online dataset, www.dlr.de.

DOD (2006). German oceanographic data centre, online dataset, www.bsh.de.

Doerfer, R., Schiller, H., and Peters, M. (2006). Meris regional case 2 water algorithms (c2r). http://www.brockmann-consult.de/beam/software/plugins/merisc2r-1.1.

Doerffer, R. and Fischer, J. (1994). Concentrations of chlorophyll, suspended matter and gelbstoff in case-ii waters derived from satellite coastal zone colour scanner data with inverse modeling methods. *J Geoph Res*, 99:745–746.

Dyer, K., Cornelisse, J., Dearnaley, M., Fennessy, M., S.E.Jones, Kappenberg, J., McCave, I., Perjrup, M., andW. van Leussen, W. P., and Wolfstein, K. (1996). A comparison of in situ techniques for estuarine flock settling velocity measurements. *Journal of Sea Research*, 36(1/2):15–29.

Eisma, D. and Kalf, J. (1987). Distribution, organic content and particle size of suspended matter in the North Sea. *Netherlands Journal of Sea Research*, 21 (4):265–285.

Feser, F., Weisse, R., and von Storch, H. (2001). Multi-decadal atmospheric modeling for europe yields multi-purpose data. *EOS Transactions*, 82 28:345–402.

Fettweis, M., Nechad, B., and den Eynde, D. V. (2007). An estimate of the suspended particulate matter (SPM) transport in the southern North Sea using SeaWiFS images, in situ measurements and numerical model results. *Continental Shelf Research*, 27(10-11):1568–1583.

Gayer, G., Dick, S., Pleskachevsky, A., and Rosental, W. (2004). Modellierung von schwebstofftransporten in Nordsee und Ostsee. Berichte des BSH 36, BSH, Hamburg.

Gayer, G., Dick, S., Pleskachevsky, A., and Rosenthal, W. (2006). Numerical modeling of suspended matter transport in the North Sea. *Ocean Dynamics*, 56:62–77.

GRDC (2006). Global runoff data centre, online dataset, http://grdc.bafg.de.

Günther, H., Hasselmann, S., and Janssen, P. (1992). The WAM model cycle 4. Technical Report 4, Deutsches Klimarechen-zentrum, Hamburg.

Haarich, M., Kienz, W., Krause, M., and Schmidt, G.-P. Z. D. (1993). Heavy metal distribution in different compartments of the northern North Sea and adjacent areas. *Ocean Dynamics*, 45(5):313–336.

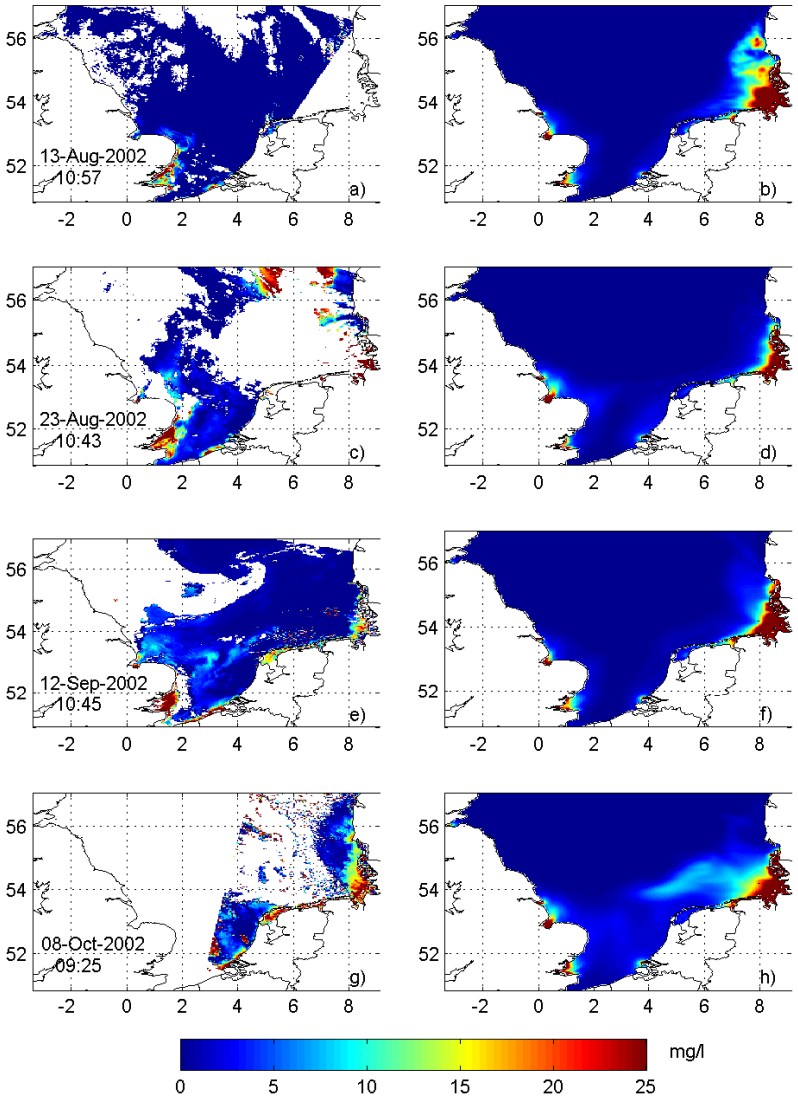

Figure 16: Surface SPM concentration (mg l^{-1}) in the North Sea calculated from MERIS data (left) and by the model (right) in August, September and October 2002.

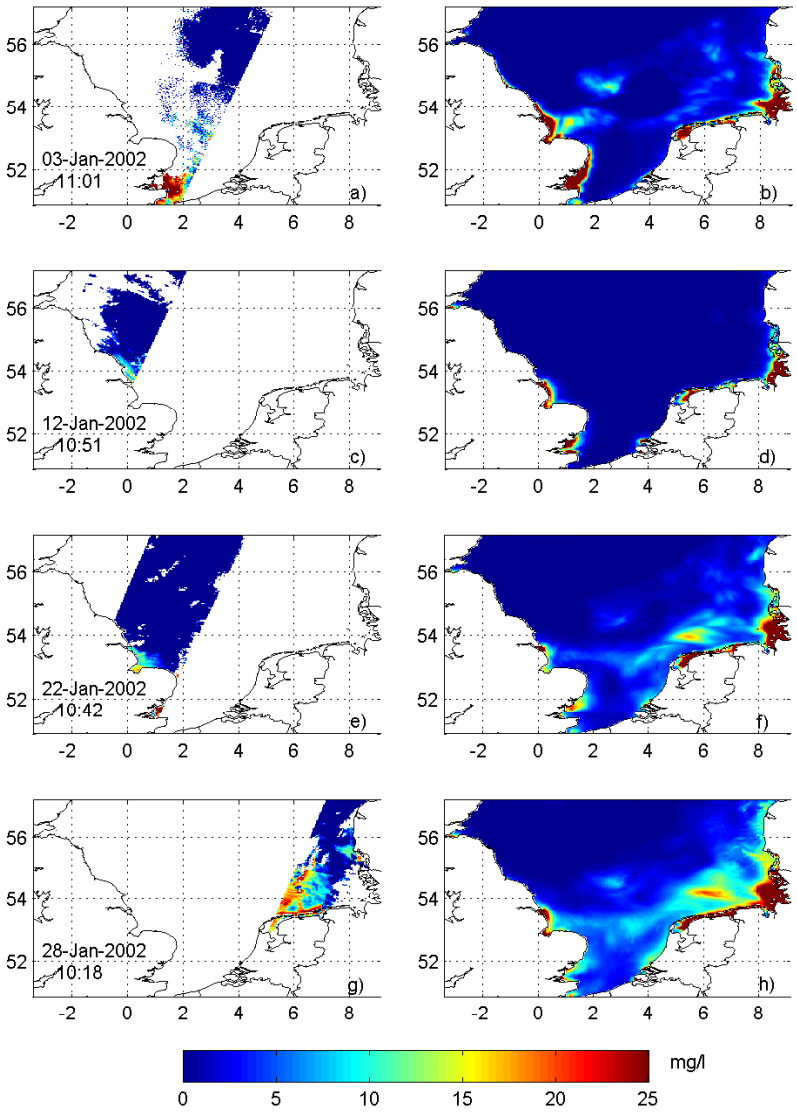

Figure 17: Surface SPM concentration (mg l^{-1}) in the North Sea calculated from MOS data (left) and by the model (right) in January 2002.

Hirota, J. and Szyper, J. P. (1975). Separation of total particulate carbon into inorganic and organic components. *Limnology and Oceanography*, 20:896–899.

Huang, D., Su, J., and Backhaus, J. (1999). Modelling the seasonal thermal stratification and baroclinic circulation in the Bohai Sea. *Continental Shelf Research*.

Ilyina, T., Pohlmann, T., Lammel, G., and Sündermann, J. (2006). A fate and transport ocean model for persistent organic pollutants and its application to the North Sea. *Journal of Marine Systems*, 63(1-2):1–19.

Jonasz, M. and Fournier, G. R. (2007). *Theoretical and Experimental Foundations Light Scattering by Particles in Water*. Elsevier.

Koenig, P., Frohse, A., and Klein, H. (1994). Measurements of the suspended matter dynamics in the German Bight. In Sündermann, J., editor, *Circulation and Contaminant Fluxes in the North Sea*, pages 250–270. Springer Verlag.

Komen, G., Cavaleri, L., Donelan, M., Hasselmann, K., Hasselmann, S., and Janssen, P. (1994). *Dynamics and Modelling of Ocean Waves*. Cambridge University Press.

Krumbein, W. C. and Sloss, L. L. (1963). *Stratigraphy and Sedimentation, 2nd edition*. Freeman, San Francisco.

Lenhart, H. J. and Pohlmann, T. (1997). The ices-boxes approach in relation to results of a north sea circulation model. *Tellus*, 49A:139–160.

Moll, A. (1998). Regional distribution of primary production in the North Sea simulated by a three-dimensional model. *Journal of Marine Systems*, 16:151–170.

NCEP (2005). National centers for environmental prediction, online dataset, http://www.ncep.noaa.gov.

Nies, H., Harms, I., Karcher, M., Dethleff, D., and Bahe, C. (1999). Anthropogenic radioactivity in the Arctic Ocean - review of the results from the joint german project. *The Science of the Total Environment*, 237(238):181191.

Pätsch, J. and Lenhart, H.-J. (2004). *Daily Loads of Nutrients, Total Alkalinity, Dissolved Inorganic Carbon and Dissolved Organic Carbon of the European continental rivers for the years 1977-2002.*, page 159. Number 48 in Berichte aus dem Zentrum für Meeres- und Klimaforschung, Reihe B: Ozeanographie.

Pleskachevsky, A., Gayer, G., Horstmann, J., and Rosenthal, W. (2005). Synergy of satellite remote sensing and numerical modelling for monitoring of suspended particulate matter. *Ocean Dynamics*, 55(1):2–9.

Pohlmann, T. (1996). Predicting the thermocline in a circulation model of the North Sea. parti: Model description, calibration, and verification. *Cont Shelf Res*, 7:131–146.

Pohlmann, T. (2006). A meso-scale model of the central and southern North Sea: Consequences of an improved resolution. *Continental Shelf Research*, 26:2367–2385.

Pohlmann, T. and Puls, W. (1994). Currents and transport in water. In Sündermann, J., editor, *Circulation and Contaminant Fluxes in the North Sea*, pages 345–402. Springer Verlag.

Puls, W. (2006). Personal communication.

Puls, W., Kuehl, H., Frohse, A., and Koenig, P. (1995). Measurements of the suspended matter settling velocity in the German Bight (North Sea). *Deutsche Hydrographische Zeitschrift*, 47 (4):259–276.

Puls, W., Pohlmann, T., and Suendermann, J. (1997). Suspended particulate matter in the southern north sea: Application of anumerical model to extend NERC North Sea project data interpretation. *German Journal of Hydrography*, 49 Number 2/3:307–327.

Reid, P., Lancelot, C., Gieskes, W., Hagmeier, E., and Weichart, G. (1990). Phytoplankton in the North Sea and its dynamics: A review. *Netherlands Journal of Sea Research*, 26(2-4):295–331.

Schrum, C. (2001). Regionalization of climate change for the North Sea and Baltic Sea. *Climate Research*, 18(1/2):31–37.

Seifert, T., Fennel, W., and Kuhrts, C. (2009). High resolution model studies of transport of sedimentary material in the south-western baltic. *Journal of Marine Systems*, 75:382–396.

Siegel, H., Gerth, M., Heene, T., Ohde, T., Rüß, D., and Kraft, H. (2009). Hydrography, currents and distribution of suspended matter during a dumping experiment in the western Baltic Sea at a site near Warnemünde. *Journal of Marine Systems*, 75:397–408.

Soulsby, R. (1997). *Dynamics of marine sands. A manual for practical application.* Thomas Telford Services, London.

Stanev, E., Dobrynin, M., Pleskachevsky, A., and Grayek, S. (2009). Bed shear stress in the southern north sea as an important driver for suspended sediment dynamics. *Ocean Dynamics*, 59:183–194.

Strickland, J. and Parsons, T. (1998). *A practical Handbook of Sea Water Analysis*, chapter 8, pages 181–184. Unipub.

Sündermann, J. and Puls, W. (1990). Modelling of suspended sediment dispersion and related transport of lead in the north sea. *Mitt. Geol.-Paläont. Institut Univ. Hamburg*, 69:143–155.

WAMDI Group (1988). The WAM Model-A third generation ocean wave prediction model. *Journal of Physical Oceanography*, 18, Issue 12:1775–1810.

Wentworth, C. K. (1922). A scale of grade and class terms for clastic sediments. *Journal of Geology*, 30(9):377–392.